MODELLING OF INDOOR WIRELESS PROPAGATION AND COMPARING THE RESULTS WITH FEKO

by
Didem Müftüoğlu

Submitted to the Institute of Graduate Studies in
Science and Engineering in partial fulfillment of
the requirements or the degree of
Master Science
in
Electrical and Electronics Engineering

Yeditepe University
2010

MODELLING OF INDOOR WIRELESS PROPAGATION AND COMPARING THE RESULTS WITH FEKO

APPROVED BY:

Inst. Dr. Cahit CANBAY
(Supervisor)

Prof. Dr. Hüseyin Selçuk VAROL

Asst. Prof. Dr. Aktül KAVAS

DATE OF APPROVAL: ……/……/…….

ACKNOWLEDGEMENTS

Firstly, I want to thank to my family for their positive encouragement.

I would like to thank to my supervisor Inst. Dr. Cahit Canbay for his great help, guidance, advices, criticism and positive encouragement. I also would like to thank to İlhami Ünal for his help for simulation and guidance.

ABSTRACT

MODELLING OF INDOOR WIRELESS PROPAGATION AND COMPARING THE RESULTS WITH FEKO

In this work, indoor wireless propagation is studied. It is hard to solve indoor wireless propagation problems by analytical methods. In order to solve this problem, an office room is modelled; and simulation and experimental results are compared to each other. The model was constructed like a real office room and suitable for the electromagnetic theory.

The practical study is divided into three parts. First part is free office room (without furniture), second part is furniture located in the office, which is made of cartoon (cartoons dielectric properties similar to the wood). Third part is cartoon furniture located in the office, which is covered by aluminum foil. Also at the second and third parts, there exist two water bottles as a model of human and child, which is filled with sea water and drinking water mixtures. All the measurements are made both by using Transverse Electric and Transverse Magnetic modes.

In conclusion, with simulation program the modelled same office room is analyzed to compare with the measurement results of free office room, office room filled with cartoon furniture and office room filled metal furniture. It is observed that practical solutions can not be the same with simulation results.

ÖZET

KAPALI ORTAMLARDA KABLOSUZ İLETİŞİM' İN MODELLENMESİ VE ÖLÇÜM SONUÇLARININ FEKO SİMÜLASYON PROGRAM SONUÇLARI İLE KARŞILAŞTIRILMASI

Bu çalışma da, kapalı ortamlarda kablosuz iletişim'in yayılma sonuçları üzerinde durulmuştur. Kapalı ortamlardaki kablosuz iletişim yayılma sonuçlarını analitik olarak çözmek nerdeyse imkansızdır. Bu sebepten dolayı çalışmamda, elektromagnetik teoriye ve gerçeğe uygun model bir ofis tasarlanmış ve üzerinde çalışılmıştır. Ayrıca benzetim programında aynı ofis modellenmiş ve sonuç alınmaya çalışılmıştır.

Model ofis üzerinde üç tip senaryo belirlenmiştir. İlk senaryo da model'in içi boşaltılarak boş ofis ölçümleri yapılmıştır. İkinci senaryoda ise model içine mukavvadan yapılma ofis malzemeleri (mukavva'nın dielektrik özellikleri ağaç malzeme ile benzer olduğu için) yerleştirilmiştir. Üçüncü senaryoda ise ofis malzemelerinin tamamı alüminyum folyo ile kaplanıp ölçüm yapılmıştır. Ayrıca ikinci ve üçüncü senaryolarda insan modeli olması amacıyla yerleştirilen iki adet su şişesi bulunmaktadır, Bu su şişeleri deniz ve içme suyundan oluşan karışım ile doldurulmuştur. Bütün ölçümler yatay ve dikey polarizasyonlarda yapılmıştır.

Sonuç olarak model ve simülasyon programındaki sonuçlar karşılaştırılarak en verimli yöntemin bulunması amaçlanmıştır, simülasyon programında bu üç tip senaryo modellenmiştir.

TABLE OF CONTENTS

LIST OF FIGURES

LIST OF TABLES

LIST OF SYMBOLS / ABBREVIATIONS

BSC	Base Station Controller
CAD	Computer-Aided Design
cm	Centimeter
GHz	Gigahertz (thousands of MHz)
GPRS	General Packet Radio Service
GSM	Global System for Mobile communications
H.W.D.A	Half Wave Dipole Antenna
Hz	Hertz (formerly cycles per second)
KHz	Kilohertz
LOS	Line of Sight
m	Meter (SI unit of length)
MHz	Megahertz (million Hertz)
MSC	Mobile Switching Centre
OBS	Obstructed Of Sight
PCS	Personal Communication Systems
PL	Path Loss
RMS	Root Mean Square
WLAN	Wide Local Area Network
2G	Second Generation
3G	Third Generation
C	Fresnel cosine integral
E	Electric field
E_i	Incident wave
E_r	Reflected wave
H	Magnetic field
n_1	Refractive Indice 1
n_2	Refractive Indice 2
S	Fresnel sine integral
TE	Transverse electric

TM	Transverse magnetic
Tx	Transmitter
Rx	Receiver
Q_n	nth correction factor
$\Gamma_{//}$	Reflection coefficient for parallel polarization
$\Gamma_{\perp}$	Reflection coefficient for perpendicular polarization
γ	Penetration (skin depth)
ε_1	Relative Permittivity 1
ε_2	Relative Permittivity 2
η_1	Characteristic Impedance 1
η_2	Characteristic Impedance 2
θ_i	Incident electromagnetic wave angle
θ_r	Reflected electromagnetic wave angle
θ_t	Refracted electromagnetic wave angle
λ	Wavelength
μ_1	Permeability 1
μ_2	Permeability 2
σ_1	Conductivity 1
σ_2	Conductivity 2
ω	Angular frequency

1. INTRODUCTION

The growing demand of mobile cellular telephony, especially in densely populated urban areas, and spectrum limitation mean that smaller and smaller cells are necessary. In the planning of micro and picocells, the knowledge of the signal coverage must be as precise as possible. In addition, the flexibility achieved by the elimination of cabling has led to new services and wireless communication systems of increasing bandwidth. The design, planning, and installation of this kind of wideband service, on the one hand, and research into future applications of wireless local area networks (WLANs) and personal communication systems (PCSs), on the other, require CAD tools not only to calculate coverage, but also to estimate radio-channel performance.

A pico-cell base-station is usually installed inside a building providing coverage also outside around the building. Drop calls of mobile communication operators in closed platforms (e.g., corridors, elevators, underground and metro stations) have been carried out very importantly for last five years. Customers want to talk without drop at any location. Indoor wireless systems, as well as the third-generation (3G) and beyond mobile communication services, can provide large bandwidth and user capacity to highly localized areas.

The cellular planning of these new systems is affected by two major factors. First, users operate in different and changing environments, from ground level in the street to the top floor in a modem office building. Secondly, a good level of coverage must be guaranteed in both indoor and outdoor environments. It is therefore necessary to develop engineering tools that can simultaneously analyze propagation and radio-channel performance in three dimensional outdoor and indoor cells.

In-building systems are an essential component of most wireless systems. They provide the following benefits: improved coverage in the locations where hot spots of traffic occur, such as airports and shopping centers; focused capacity for these large public hot spots; flexible tariffs and wireless services for corporate offices and excellent control

of interference and wideband channel dispersion for high data - rate systems. Despite having a fixed building geometry, this control of interference is possible by selecting antenna locations appropriately, taking into account building partitions and openings, therefore coverage is maximized in the desired directions, and cell footprint can be shaped more accurately, hence reducing interference with adjacent cells. Today, many technologies require the deployment of such systems, including second generation (2G) and third generation (3G) cellular, TETRA and wireless LAN (WLAN). WLAN systems in particular have been responsible for an explosive growth in the number of in-building systems in the last year, while 3G is already starting to stimulate new in-building systems to realize its highest data rate potential. For systems based on TETRA, in-building systems are helping to provide safe policing and management of public and private buildings. To design these systems effectively and economically, system designers need processes and tools which can provide a high level of confidence in the designs [1].

Indoor propagation modeling is demanded for the design and the maintenance of indoor wireless services. For the design and maintenance of indoor wireless services the knowledge of the signal propagation in different environments is demanded. Indoor propagation is one of the most complicated propagation topics based on the specific type of building structure and used materials. Empirical modeling based on statistics seems to be the most efficient approach since there is no need of precise definition of the building interiors. On the other hand, such models can failed indoor situations where more precise model should be used e.g. ray tracing [2].

With the growing dependence on computers, communication and control equipment the problem of sensitivity to interference becomes more apparent. Therefore we need Electromagnetic Compatibility for the equipments which are electronic devices. Electromagnetic Compabtility (EMC) is the ability of a device to operate faultlessly in a prescribed electromagnetic environment without at the same time affecting its surroundings in an inadmissible way. EMC also affects human health; therefore all machines must work with the frequency in order not to affect human health [3].

By the way, in this study an office room is modelled and simulated by using electromagnetic modeling techniques in electromagnetic theory. The model was

constructed like a real office (with appropriate dimensions for electromagnetic modeling) for practical measurements. Simulation and experimental results are compared to each other.

The practical study is divided into three parts. First part is free office room (without furniture), second part is furniture located in the office, which is made of cartoon (cartoons dielectric properties similar to the wood). Third part is cartoon furniture located in the office, which is covered by aluminum foil. Also at the second and third parts, there exist two water bottles as a model of human and child, which is filled with sea water and drinking water mixtures. All the measurements are made both by using Transverse Electric (TE) and Transverse Magnetic (TM) modes.

With the simulation program, the same office room is modeled to get measurement results of free office, office filled with cartoon furniture, and office filled metal furniture. All of these measurements are also taken by the simulation program both by using Transverse Electric (TE) and Transverse Magnetic (TM) modes.

In conclusion, it is hard to explain indoor propagation by analytical expressions. The future comes to the centre of our life by “wireless propagation”. Therefore, we used numerical simulation programs and we made measurements in real buildings in order to get true results.

2. INDOOR PROPAGATION

Indoor propagation is wireless communication system typically covering a small area, such as in-building (offices, shopping malls, train stations, etc.), or more recently in-aircraft. Another meaning of the indoor propagation is picocell. A picocell is analogous to a WLAN access point.

In cellular wireless networks, such as GSM, the picocell base station is typically a low cost, small (typically the size of a sheet of A4 paper and about 2-3 cm thick), reasonably simple unit that connects to a Base Station Controller (BSC). Multiple picocell 'heads' connect to each BSC: the BSC performs radio resource management and hand-over functions, and aggregates data to be passed to the Mobile Switching Centre (MSC) and/or the GPRS Support Node (GSN).

Connectivity between the picocell heads and the BSC typically consists of in-building wiring. Although originally deployed systems (1990s) used PDH links such as E1/T1 links, more recent systems use Ethernet cabling.

More recent work has developed the concept towards a head unit containing not only a picocell, but also many of the functions of the BSC and some of the MSC. This form of picocell is called an access point base station or fem to cell. In this case, the unit contains all the capability required to connect directly to the Internet, without the need for the BSC/MSC infrastructure. This is potentially a more cost effective approach.

In cellular networks, picocells are typically used to extend coverage to indoor areas where outdoor signals do not reach well, or to add network capacity in areas with very dense phone usage, such as train stations [4].

3. PROPERTIES OF INDOOR PROPAGATION

Indoor channels are different from traditional mobile radio channels in two different ways:

I. The distances covered are much smaller

II. The variability of the environment is much greater for a much smaller range of Tx - Rx separation distances.

The propagation inside a building is influenced by:

- Layout of the building
- Construction materials
- Building type: sports arena, residential home, factory

Indoor propagation is domited by the same mechanisms as outdoor: reflection, scattering, diffraction.

- However, conditions are much more variable
- Doors/windows open or not
- The mounting place of antenna: desk, ceiling, etc.
- The level of floors

Indoor channels are classified as

- Line-of-sight (LOS)
- Obstructed (OBS) with varying degrees of clutter [5].

4. BUILDING TYPES

The most important things for the indoor propagation are building types, material types, geometry and architecture. The thickness of the exterior walls, thickness of the interior walls, material type of the building materials, thickness of the ceilings, thickness of the floors are related with the propagation factor. Each type of the buildings has their own material and architectural property.

There are some important building types.

- Residential homes in suburban areas
- Residential homes in urban areas
- Traditional office buildings with fixed walls (hard partitions)
- Open plan buildings with movable wall panels (soft partitions)
- Factory buildings
- Grocery stores
- Retail stores
- Sport areas

5. PROPAGATION MECHANSIMS

5.1. REFLECTION

Reflection occurs when a propagating electromagnetic wave impinges upon an object which has very large dimensions when compared to the wavelength of the propagating wave. Reflections occur from the surface of the earth and form building and walls.

When a radio wave propagating in one medium impinges upon another medium having different electrical properties, the wave is partially reflected and partially transmitted. If the plane wave is incident on a perfect dielectric, part of the energy is transmitted into the second medium and part of the energy is reflected back into the first medium, and there is no loss of energy in absorption. If the second medium is a perfect conductor, then all incident energy is reflected back into the first medium without loss of energy. The electric field intensity of the reflected and transmitted waves may be related to the incident wave in the medium of origin through the Fresnel reflection coefficient. The reflection coefficient is a function of the material properties, and generally depends on the wave polarization, angle of incidence, and the frequency of the propagating wave [6].

5.1.1. Reflection from Dielectrics

Figure 5.1 shows an electromagnetic wave incident at an angle θ_i with the plane of the boundary between two dielectric media. As shown in the figure, part of the energy is reflected back to the first media at an angle θ_r and part of the energy is refracted into the second media at an angle θ_t. The nature of reflection varies with the direction of polarization of the electric field.

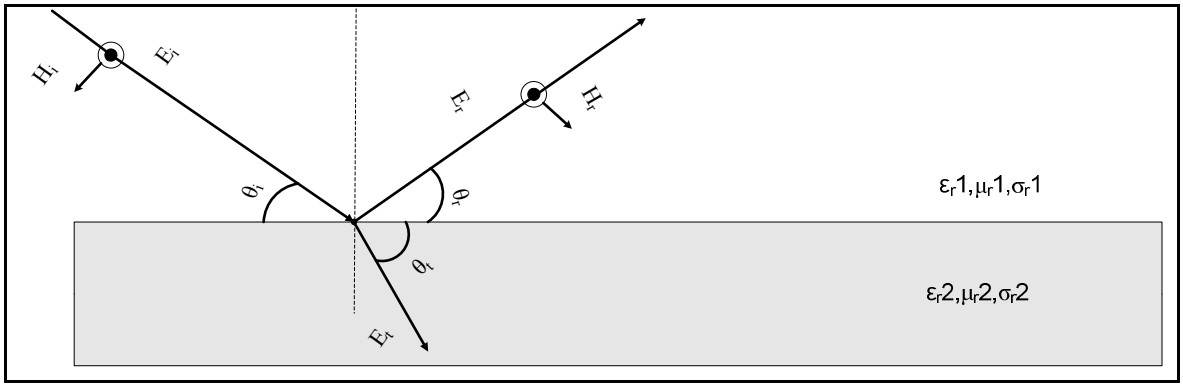

Figure 5.1. Electric field in the plane of incidence TE polarization [6]

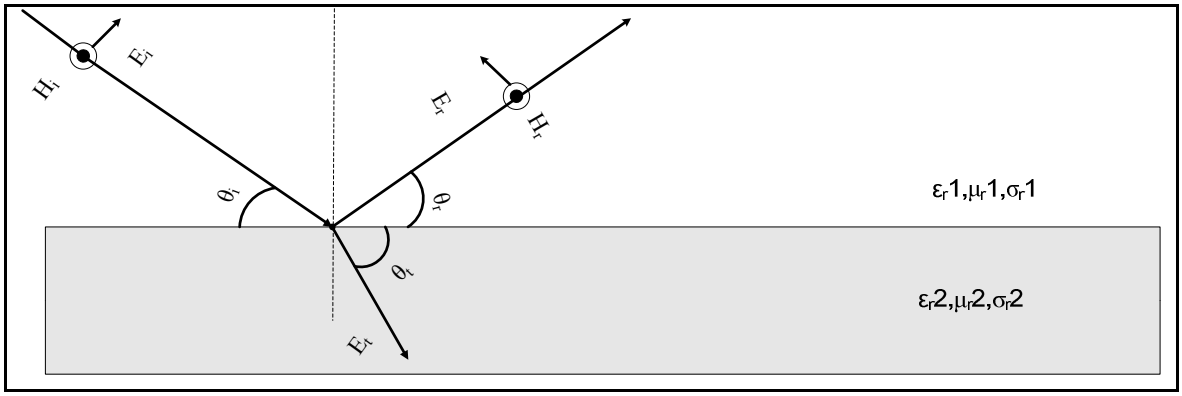

Figure 5.2. Electric field in the plane of incidence TE polarization [6]

In Figure 5.1, the parameters represent medium parameters. Parameters ε_1, ε_2 are relative permittivities; μ_1, μ_2 represent permeabilities, and σ_1, σ_2 represent conductivities [9].

Because of superposition, only two orthogonal polarizations need be considered to solve general reflection problems. The reflection coefficients ($\Gamma_{\parallel}$, $\Gamma_{\perp}$) for the two cases of parallel (TM) and perpendicular (TE) E-field polarization at the boundary of two dielectrics are given by,

$$\eta_1 = \sqrt{\frac{\mu_1}{\varepsilon_1}} \tag{5.1}$$

$$\eta_2 = \sqrt{\frac{\mu_2}{\varepsilon_2}} \tag{5.2}$$

$$\Gamma_{\parallel} = \frac{E_r}{E_i} = \frac{\eta_2 \sin\theta_t - \eta_1 \sin\theta_i}{\eta_2 \sin\theta_t + \eta_1 \sin\theta_i} \tag{5.3}$$

$$\Gamma_{\perp} = \frac{E_r}{E_i} = \frac{\eta_2 \sin\theta_i - \eta_1 \sin\theta_t}{\eta_2 \sin\theta_i + \eta_1 \sin\theta_t} \tag{5.4}$$

Using the MATHCAD simulation program, reflection model for the walls ceramic and wood is studied. Operation frequency is 9.4 GHz. My model has two kind of wall type. First type is wooden wall, εr = 2.9, μr = 1, σ = 0.286. Second type is ceramic wall, εr = 5.5, μr = 1, σ = 3.75. Distance d = 1.2 m. Transmitter antenna height ht = 0.57 m. Receiver antenna heights are hr = 0.18 m and 0.34 m. I assume that walls are infinitely long, because it is hard to simulate finite materials.

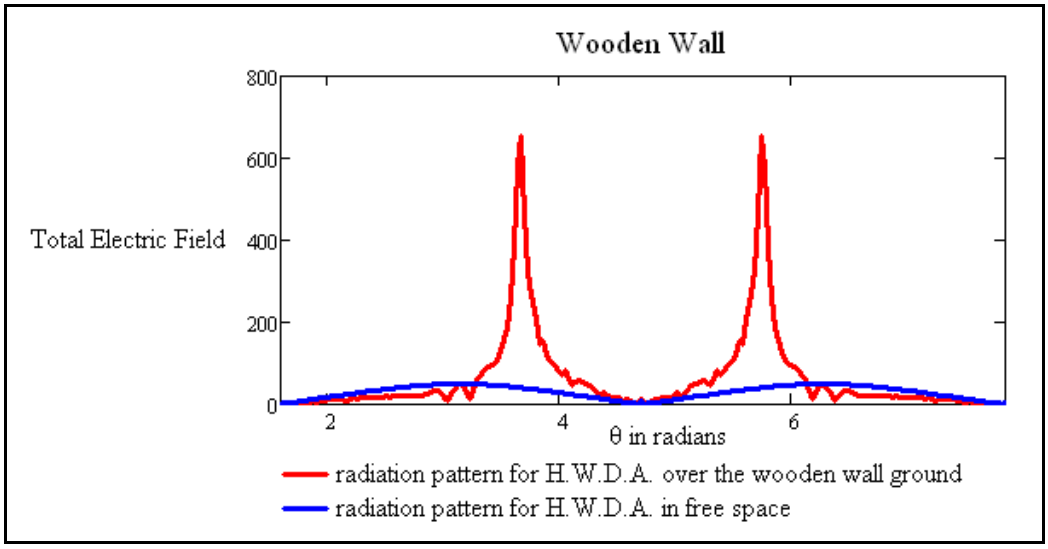

Figure 5.3. Effects of the reflection from infinite wooden wall at TM mode

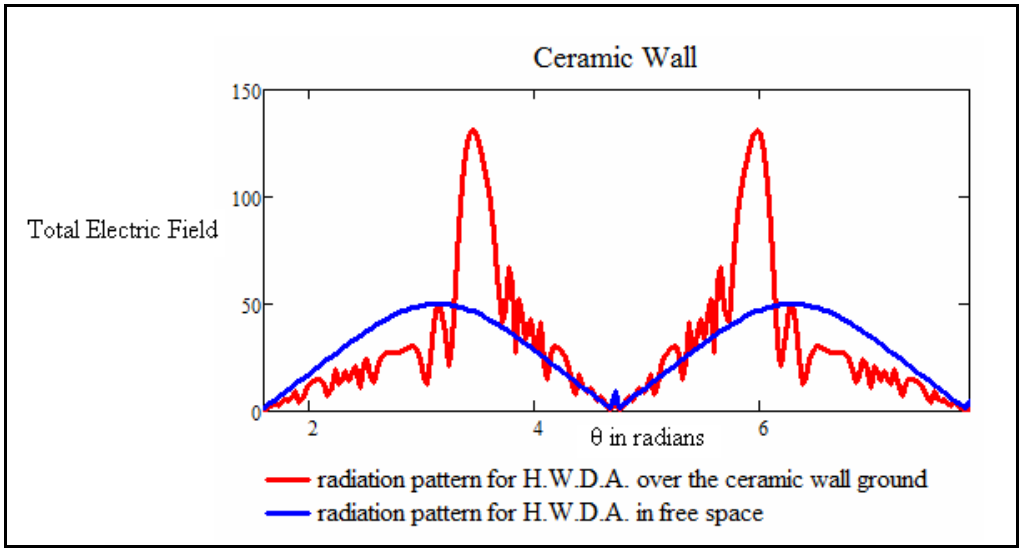

Figure 5.4. Effects of the reflection from infinite ceramic wall at TM mode

5.1.1.1. Ground Waves

The ground wave is actually composed of two separate component waves. These are known as the Surface Wave and the Space Wave. The determining factor in whether a ground wave component is classified as a space wave or a surface wave is simple. A surface wave travels along the surface of the Earth. A space wave travels over the surface [7].

5.1.1.2. Surface Waves

The surface wave reaches the receiving site by traveling along the surface of the ground as shown in In Figure 5.5 and 5.6. A surface wave can follow the contours of the Earth because of the process of diffraction. When a surface wave meets an object and the dimensions of the object do not exceed its wavelength, the wave tends to curve or bend around the object. The smaller the object, the more pronounced the diffractive action will be. Most long-distance LF "longwave" radio communication (between 30 kHz and 300 kHz) is a result of groundwave propagation [7].

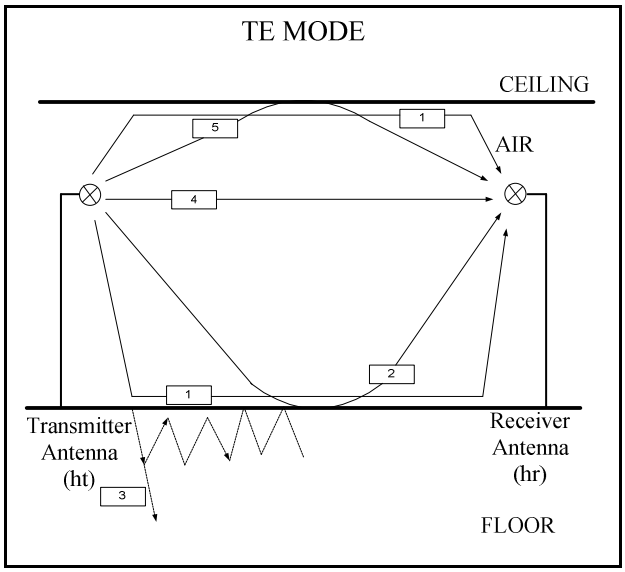

Figure 5.5. Way to reach from transmitter to receiver antenna at TE Mode [8]

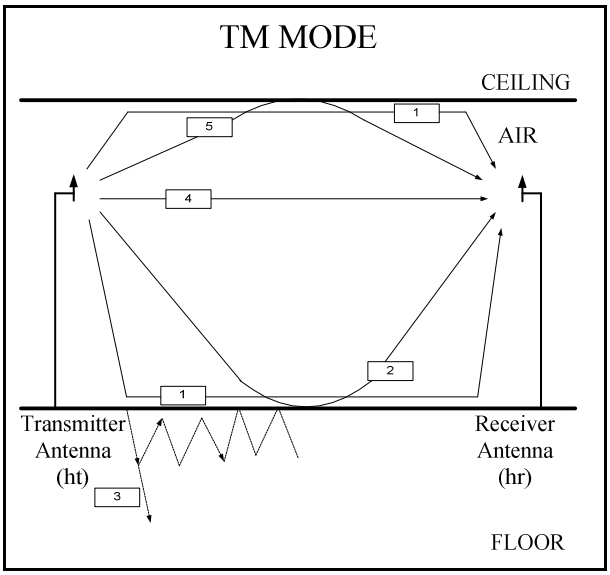

Figure 5.6. Way to reach from transmitter to receiver antenna at TM Mode [8]

From the Figure 5.5 above, definitions of the ways [8];

1. Surface Wave
2. Space Wave
3. Lateral Wave
4. Space Wave
5. Sky Wave

5.1.2. Reflection from Perfect Conductors

Since electromagnetic energy cannot pass through a perfect conductor a plane wave incident on a conductor has all its energy reflected. As the electric field at the surface of the conductor must be equal to zero at all times. Reflected wave must be equal in magnitude to the incident wave [9].

$$\theta_i = \theta_r \tag{5.5}$$

$$E_i = E_r \tag{5.6}$$

When the electric field is horizontally polarized, the boundary conditions require that;

$$E_i = -E_r \tag{5.6}$$

From the equations (5.5), (5.6) for a perfect conductor, $\Gamma_{\parallel} = 1$, and $\Gamma_{\perp} = -1$.

5.2. CORRECTION FACTOR

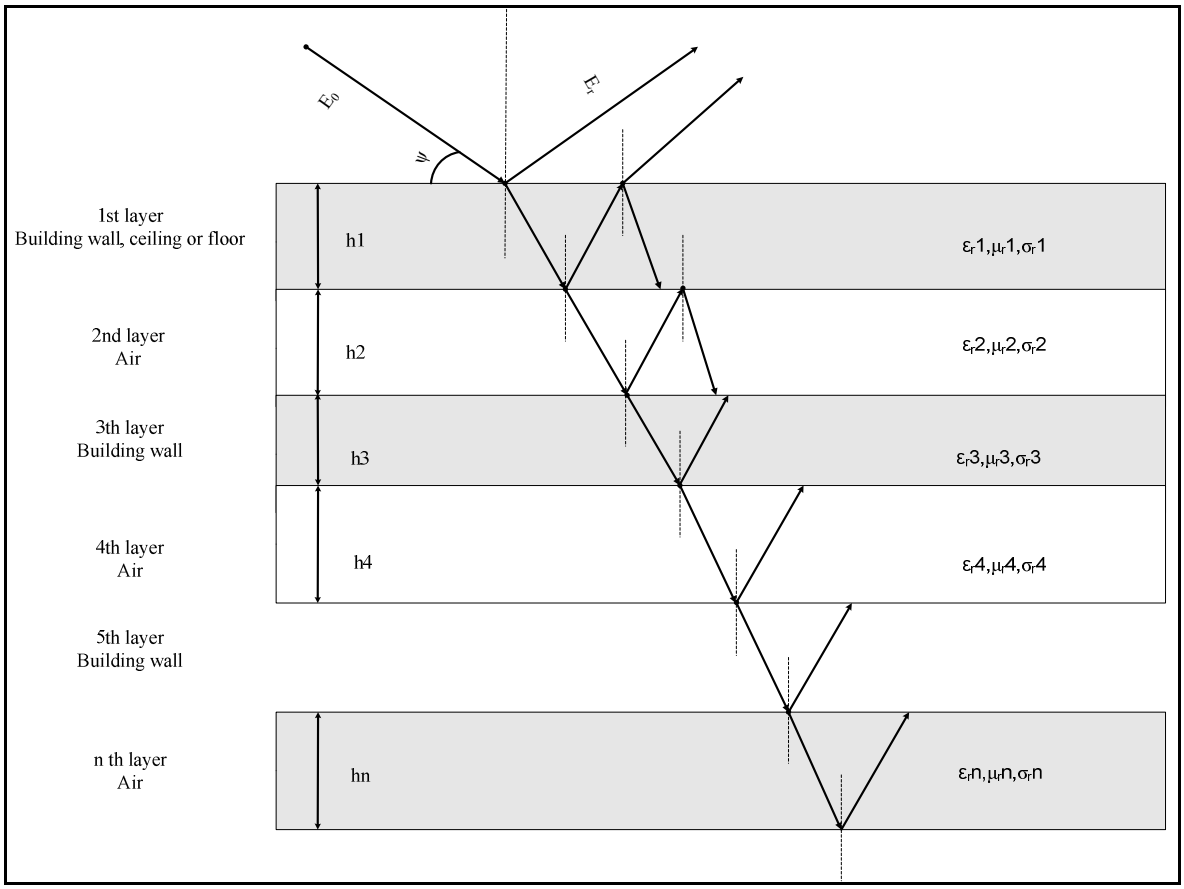

Figure 5.7. N- Layered dispersive lossy planar media [8]

Computation of reflection coefficient from n-layered dispersive lossy planar media illuminated by plane waves for both TE and TM modes can be obtained by using the following quality factor. Classical methods using boundary conditions has been applied for the theoretical derivation.

$$Q4 = \frac{1 + \frac{\gamma 5}{\gamma 4}\tanh(\gamma 4 * h4)}{\frac{\gamma 5}{\gamma 4} + \tanh(\gamma 4 * h4)} \tag{5.7}$$

$$Q3 = \frac{Q4 + \frac{\gamma 4}{\gamma 3}\tanh(\gamma 3 * h3)}{\frac{\gamma 4}{\gamma 3} + \tanh(\gamma 3 * h3)} \tag{5.8}$$

$$Q2 = \frac{Q3 + \frac{\gamma 3}{\gamma 2}\tanh(\gamma 2 * h2)}{\frac{\gamma 3}{\gamma 2} + \tanh(\gamma 2 * h2)} \tag{5.9}$$

$$Q1 = \frac{Q2 + \frac{\gamma 2}{\gamma 1}\tanh(\gamma 1 * h1)}{\frac{\gamma 2}{\gamma 1} + \tanh(\gamma 1 * h1)} \tag{5.10}$$

$$Reflection = \frac{Z_1 - 120\pi}{Z_1 + 120\pi} \tag{5.10}$$

$$Z_1 = Q_1 * \eta_1 \tag{5.11}$$

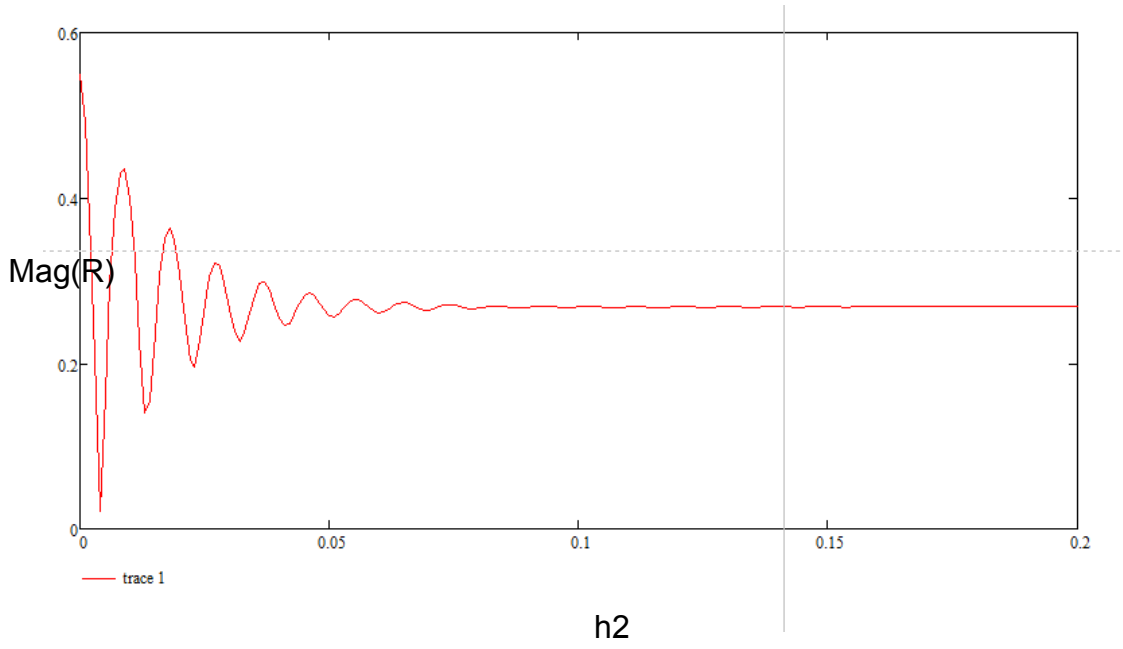

Figure 5.8. Variation of magnitude of reflection coefficient from five-layered dispersive media with respect to the depth of the second layer

From the Figure 5.8, h2 is depth of the second layer.

$$\vec{E}_0 = \vec{a}_z \left(e^{-jk_0\left(x\cos(\psi)-y\sin(\psi)\right)} + R_0\, e^{-jk_0\left(x\cos(\psi)+y\sin(\psi)\right)} \right) \tag{5.12}$$

$$\vec{E}_1 = \vec{a}_z \left(T_1\, e^{-jk_1\left(x\cos(\theta_{t1})-y\sin(\theta_{t1})\right)} + R_1\, e^{-jk_1\left(x\cos(\theta_{t1})+y\sin(\theta_{t1})\right)} \right) \tag{5.13}$$

$$\vec{E}_2 = \vec{a}_z \left(T_2\, e^{-jk_2\left(x\cos(\theta_{t2})-y\sin(\theta_{t2})\right)} + R_2\, e^{-jk_2\left(x\cos(\theta_{t2})+y\sin(\theta_{t2})\right)} \right) \tag{5.14}$$

$$\vec{E}_3 = \vec{a}_z \left(T_3\, e^{-jk_3\left(x\cos(\theta_{t3})-y\sin(\theta_{t3})\right)} + R_3\, e^{-jk_3\left(x\cos(\theta_{t3})+y\sin(\theta_{t3})\right)} \right) \tag{5.15}$$

$$\vec{E}_4 = \vec{a}_z \left(T_4\, e^{-jk_4\left(x\cos(\theta_{t4})-y\sin(\theta_{t4})\right)} + R_4\, e^{-jk_4\left(x\cos(\theta_{t4})+y\sin(\theta_{t4})\right)} \right) \tag{5.16}$$

$$\vec{E}_5 = \vec{a}_z \left(T_5\, e^{-jk_5\left(x\cos(\theta_{t5})-y\sin(\theta_{t5})\right)} \right) \tag{5.17}$$

Bounday Conditions;

$$\begin{aligned} \vec{E}_{0z} &= \vec{E}_{1z} \\ \vec{H}_{0x} &= \vec{H}_{1x} \end{aligned} \quad \text{At } y=-h_0 \tag{5.18}$$

$$\begin{aligned} \vec{E}_{1z} &= \vec{E}_{2z} \\ \vec{H}_{1x} &= \vec{H}_{2x} \end{aligned} \quad \text{At } y=-h_1 \tag{5.19}$$

$$\begin{aligned} \vec{E}_{2z} &= \vec{E}_{3z} \\ \vec{H}_{2x} &= \vec{H}_{3x} \end{aligned} \quad \text{At } y=-h_2 \tag{5.20}$$

$$\begin{aligned} \vec{E}_{3z} &= \vec{E}_{4z} \\ \vec{H}_{3x} &= \vec{H}_{4x} \end{aligned} \quad \text{At } y=-h_3 \tag{5.21}$$

$$\begin{aligned} \vec{E}_{4z} &= \vec{E}_{5z} \\ \vec{H}_{4x} &= \vec{H}_{5x} \end{aligned} \quad \text{At } y=-h_4 \tag{5.22}$$

$$k_0 \cos(\psi) = k_1 \cos(\theta_{t1}) \tag{5.23}$$

From the equations above, we can find the total field distribution at each layer [8].

5.3. REFRACTION

Refraction is the change in direction of a wave due to a change in its speed. This is most commonly observed when a wave passes from one medium to another. Refraction of light is the most commonly observed phenomenon, but any type of wave can refract when it interacts with a medium, for example when sound waves pass from one medium into another or when water waves move into water of a different depth. Refraction is described by Snell's law, which states that the angle of incidence θ_1 is related to the angle of refraction θ_2 by and n_1 and n_2 the refractive indices. In general, the incident wave is partially refracted and partially reflected; the details of this behavior are described by the Fresnel equations [10].

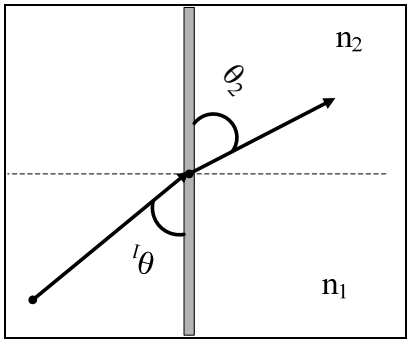

Figure 5.9. Snell's Law [8]

$$\frac{\sin\theta_1}{\sin\theta_2} = \frac{n_2}{n_1} \tag{5.24}$$

5.4. DIFFRACTION

The apparent bending of waves around small obstacles and the spreading out of waves past small openings is defined as diffraction.

Diffraction allows radio signals to propagate around the curved surface of the earth, beyond the horizon, and to propagate behind obstructions.

The phenomenon by which an electromagnetic waveform diffracts, or bends, as it strikes the sharp edge of an obstacle transverse to its direction of propagation. The portion of the signal that is not cut off by the knife edge continues to propagate, but the edge of the signal bends into the line-of-sight (LOS) shadow region as if to fill the void left by the portion of the signal cut off. Knife-edge diffraction can be used to advantage in radio communications when line-of-sight (LOS) cannot be achieved due to the presence of an obstacle, such as a mountaintop or building, that lies in the path of the transmit and receive antennas [5].

For example, in most of the offices has separated areas for workers to work comfortable. On the other hand, these separation surfaces cause diffraction. We can see in detailed from the Figure 5.4.

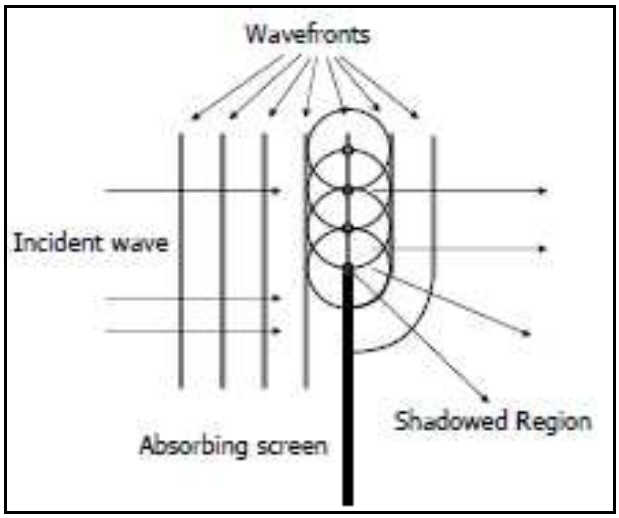

Figure 5.10. Knife edge diffraction [5]

There is two type of diffraction model;

- Knife Edge Diffraction Model
- Multiple Knife Edge Diffraction Model

The Cornu spiral is a graphical aid for evaluating the Fresnel integrals which show up in the evaluation of the diffraction intensities for the Fresnel diffraction of the light from a slit. It lends itself to the calculation of diffraction from slits, barriers, and opaque strips.

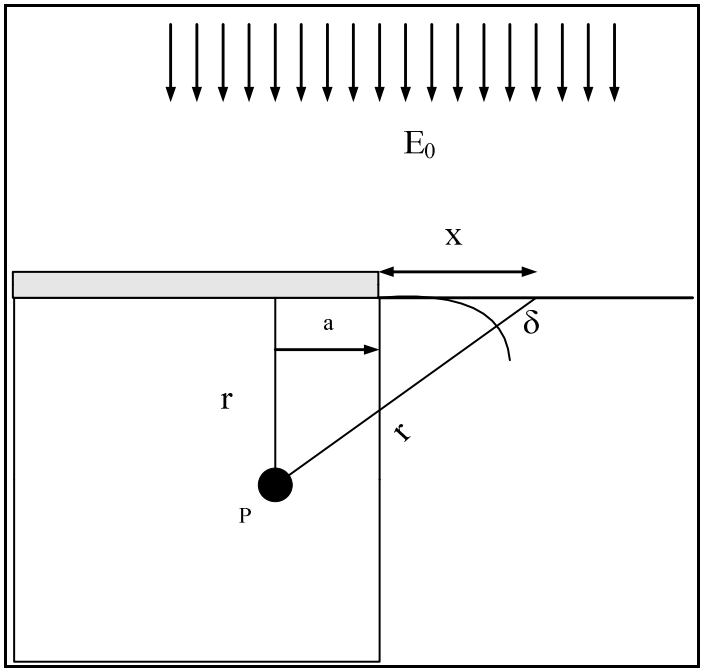

Figure 5.11. Knife edge diffraction [11]

$$E = \frac{E_0}{\kappa r} e^{-j\beta r} \int_{\kappa a}^{\infty} e^{\frac{-j\pi u^2}{2}} du \tag{5.25}$$

$$E = \frac{E_0}{\kappa r} e^{-j\beta r} \left(\int_0^{\infty} e^{\frac{-j\pi u^2}{2}} du - \int_0^{\kappa a} e^{\frac{-j\pi u^2}{2}} du \right) \tag{5.26}$$

$$E = \frac{E_0}{\kappa r} e^{-j\beta r} \left\{ \frac{1}{2} + j\frac{1}{2} - \left[C(\kappa a) + jS(\kappa a) \right] \right\} \tag{5.27}$$

$$C(\kappa a) = \int_0^{\kappa a} \cos \frac{\pi u^2}{2} du \tag{5.28}$$

$$S(\kappa a) = \int_0^{\kappa a} \sin \frac{\pi u^2}{2} du \tag{5.29}$$

Using the equations above, by the help of the Mathcad program Cornu Spiral is darwed.

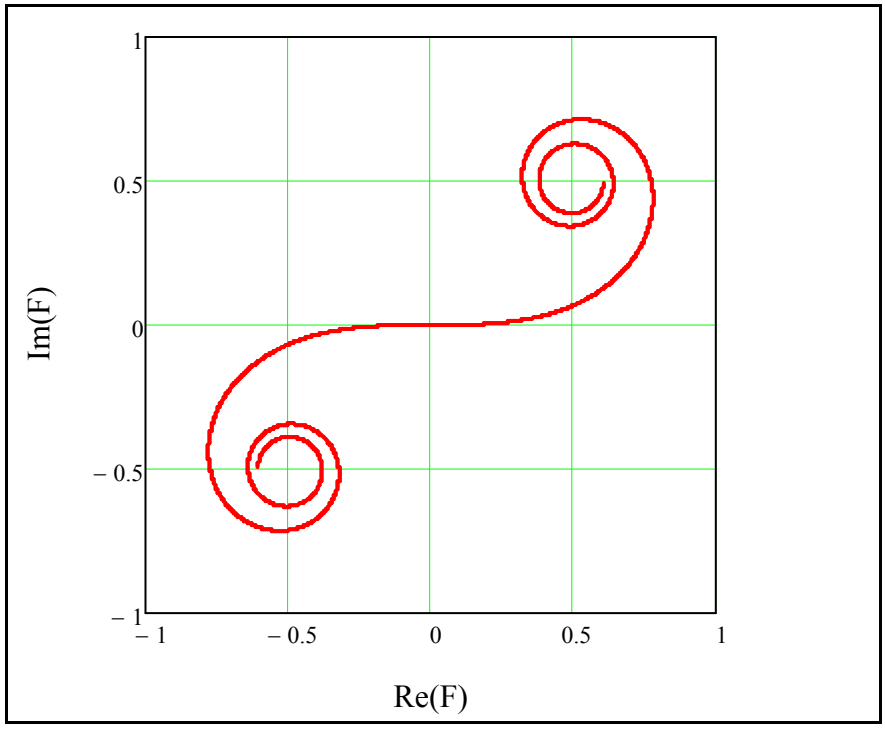

Figure 5.12. Cornu Spiral

5.5. SCATTERING

The actual received signal in a mobile radio environment is often stronger than what is predicted by reflection and diffraction models alone. This is because when a radio wave impinges on a rough surface, the reflected energy is spread out in all directions due to scattering. Objects such as lamp posts and trees tend to scatter energy in all directions, thereby providing additional radio energy at a receiver.

Flat surfaces that have much larger dimension than a wavelength may be modelled as reflective surfaces. However, the roughness of such surfaces often induces propagation effects different from the seculars reflection. Scattering from rough surfaces is much more difficult than the flat surfaces. [12].

Mie theory is used to find scattering electromangentic waves form spherical objects. Mie theory, also called Lorenz-Mie theory or Lorenz-Mie-Debye theory, is an analytical solution of Maxwell's equations for the scattering of electromagnetic radiation by spherical particles (also called Mie scattering). The Mie solution is named after its developer, German physicist Gustav Mie. However, Danish physicist Ludvig Lorenz and others independently developed the theory of electromagnetic plane wave scattering by a dielectric sphere.

The term "Mie theory" is misleading, since it does not refer to an independent physical theory or law. The phrase "the Mie solution (to Maxwell's equations)" is therefore preferable. Currently, the term "Mie solution" is also used in broader contexts, for example when discussing solutions of Maxwell's equations for scattering by stratified spheres or by infinite cylinders, or generally when dealing with scattering problems solved using the exact Maxwell equations in cases where one can write separate equations for the radial and angular dependence of solutions.

In contrast to Rayleigh scattering, the Mie solution to the scattering problem is valid for all possible ratios of diameter to wavelength, although the technique results in numerical summation of infinite sums. In its original formulation it assumed an

homogeneous, isotropic and optically linear material irradiated by an infinitely extending plane wave. However, solutions for layered spheres are also possible.

A modern formulation of the Mie solution to the scattering problem on a sphere can be found in J. A. Stratton's Electromagnetic Theory, published in 1941. In this formulation, the incident plane wave as well as the scattering field is expanded into radiating spherical vector wave functions. The internal field is expanded into regular spherical vector wave functions. By enforcing the boundary condition on the spherical surface, the expansion coefficients of the scattered field can be computed [13].

5.5.1. Scattering from Perfectly Conducting Cylinders

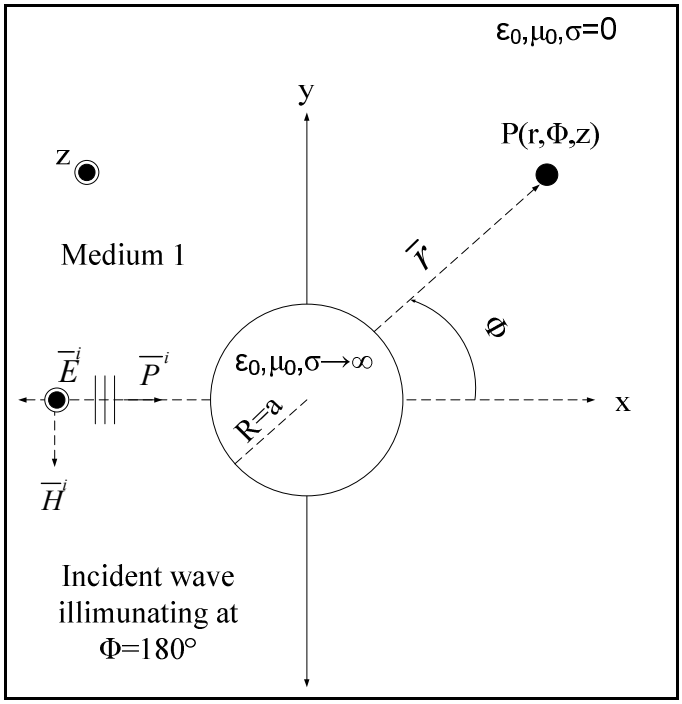

Figure 5.13. Scattering from perfectly conducting cylinder [14]

Incoming wave is defined as:

$$\vec{E}_i = e^{-jkx} = e^{-jk(r\cos(\phi))}\,\vec{a}_z \tag{5.30}$$

$$\vec{E}_i = e^{-jkx} = \sum_{n=-\infty}^{\infty} j^{-n} J_n(kr) e^{jn\phi} \vec{a}_z \tag{5.31}$$

Outward traveling wave can be expressed as:

$$\vec{E}_s = \sum_{n=-\infty}^{\infty} j^{-n} a_n H_n^{(2)}(kr) e^{jn\phi} \vec{a}_z \tag{5.32}$$

Total field is in medium1 is written as:

$$\vec{E}_T = \sum_{n=-\infty}^{\infty} j^{-n} \left(J_n(kr) + a_n H_n^{(2)}(kr) \right) e^{jn\phi} \vec{a}_z \tag{5.33}$$

Then, applying boundary conditions at r=*a*, as,

$$\vec{E}_T(r=a) = 0 \tag{5.34}$$

$$a_n = \frac{-J_n(ka)}{H_n^{(2)}(ka)} \tag{5.35}$$

$$\vec{E}_s = \sum_{n=-\infty}^{\infty} j^{-n} \left(\frac{-J_n(ka)}{H_n^{(2)}(ka)} \right) H_n^{(2)}(kr) e^{jn\phi} \vec{a}_z \tag{5.36}$$

5.5.2. Mie Scattering from Perfectly Conducting Spheres:

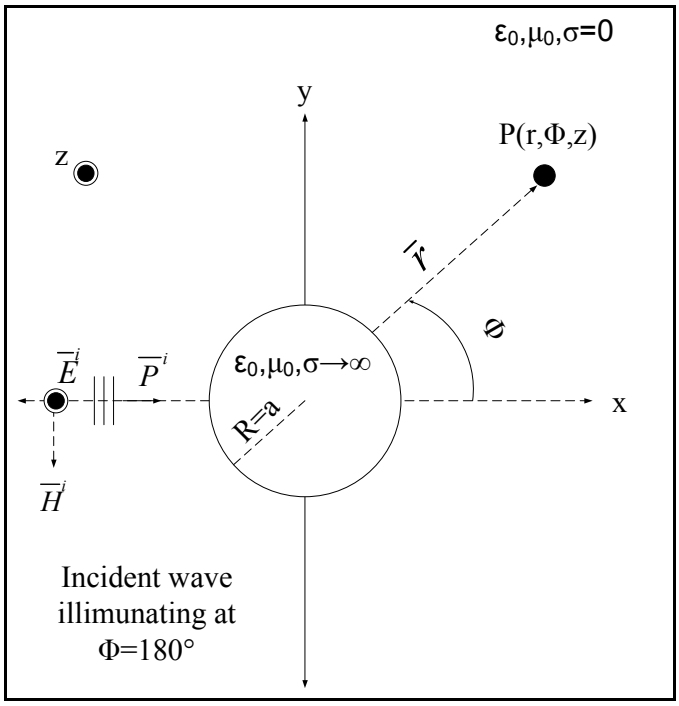

Figure 5.14. Scattering from perfectly conducting sphere [14]

$$E_{\theta s} = \frac{j E_0}{k r} e^{-jkr} \cos(\phi) \sum_{n=1}^{\infty} j^n \left[b_n \sin(\theta) P_n^{1\prime}(\cos(\theta)) - c_n \frac{P_n^1(\cos(\theta))}{\sin(\theta)} \right] \tag{5.37}$$

$$E_{\phi s} = \frac{j E_0}{k r} e^{-jkr} \sin(\phi) \sum_{n=1}^{\infty} j^n \left[b_n \frac{P_n^1(\cos(\theta))}{\sin(\theta)} - \sin(\theta) P_n^{1\prime}(\cos(\theta)) \right] \tag{5.38}$$

$$b_n = -a_n \frac{\hat{J}_n'(ka)}{\hat{H}_n^{(2)\prime}(ka)} \tag{5.39}$$

$$c_n = -a_n \frac{\hat{J}_n(ka)}{\hat{H}_n^{(2)}(ka)} \tag{5.40}$$

$$a_n = \frac{j^{-n}(2n+1)}{n(n+1)} \tag{5.41}$$

$$P_n^1\left(\cos(\theta)\right) = \frac{\partial P_n}{\partial \theta} \tag{5.42}$$

$$\hat{J}_n(kr) = kr\, j_n(kr) \tag{5.43}$$

$$E_T = \sqrt{\left|E_{\theta s}\right|^2 + \left|E_{\phi s}\right|^2} \tag{5.44}$$

Boundary conditions,

$$E_\theta = E\big|_{inside\,sphere} = 0 \tag{5.45}$$

$$E_\phi = E\big|_{inside\,sphere} = 0 \tag{5.46}$$

6. INDOOR PROPAGATION EVENTS AND PARAMETERS

With the advent of Personal Communication Systems (PCS), there is a great deal of interest in characterizing radio propagation inside buildings. The indoor radio channel differs from the traditional mobile radio channel in two aspects; the distances covered much smaller, and the variability of the environment is much greater for a much smaller range of Tx-Rx separation distances. It has been observed that propagation within buildings is strongly influenced by specific features such as the layout of the building, the construction materials, and the building type.

Indoor radio propagation is dominated by the same mechanisms as outdoor: reflection, diffraction, and scattering. However, conditions are much more variable. For example, signal levels vary greatly depending on whether interior doors are open or closed inside a building. Where antennas are mounted also impacts large-scale propagation. Antennas mounted at desk level in a partitioned office receive vastly different signals than those mounted on the ceiling. Also, the smaller propagation distances make it more difficult to insure far-field radiation for all receiver locations and types of antennas.

The field of indoor radio propagation is relatively new; with the first wave of research occurring in the early 1980's at Bell Laboratories and at British Telecom was the first to carefully study indoor path loss in and around a large number of homes and office buildings. Excellent literature surveys are available on the topic of indoor propagation. In general, indoor channels may be classified either as Line Of Sight (LOS) or obstructed (OBS), with varying degrees of clutter [9].

6.1. TEMPORAL FADING FOR FIXED AND MOVING TERMINALS

6.1.1. Fading

In wireless communications, fading is deviation of the attenuation that a carrier-modulated telecommunication signal experiences over certain propagation media. The fading may vary with time, geographical position and/or radio frequency, and is often modeled as a random process. A fading channel is a communication channel that experiences fading. In wireless systems, fading may either be due to multipath propagation, referred to as multipath induced fading, or due to shadowing from obstacles affecting the wave propagation, sometimes referred to as shadow fading.

The presence of reflectors in the environment surrounding a transmitter and receiver create multiple paths that a transmitted signal can traverse. As a result, the receiver sees the superposition of multiple copies of the transmitted signal, each traversing a different path. Each signal copy will experience differences in attenuation, delay and phase shift while travelling from the source to the receiver. This can result in either constructive or destructive interference, amplifying or attenuating the signal power seen at the receiver. Strong destructive interference is frequently referred to as a deep fade and may result in temporary failure of communication due to a severe drop in the channel signal-to-noise ratio [13].

6.1.2. Rayleigh Fading

Rayleigh fading is a statistical model for the effect of a propagation environment on a radio signal, such as that used by wireless devices.

Rayleigh fading models assume that the magnitude of a signal that has passed through such a transmission medium (also called a communications channel) will vary randomly, or fade, according to a Rayleigh distribution the radial component of the sum of two uncorrelated Gaussian random variables.

Rayleigh fading is viewed as a reasonable model for tropospheric and ionospheric signal propagation as well as the effect of heavily built-up urban environments on radio signals. Rayleigh fading is most applicable when there is no dominant propagation along a line of sight between the transmitter and receiver. If there is a dominant line of sight, Rician fading may be more applicable [15].

6.1.3. Rician Fading

Rician fading is a stochastic model for radio propagation anomaly caused by partial cancellation of a radio signal by itself the signal arrives at the receiver by two different paths (hence exhibiting multipath interference), and at least one of the paths is changing (lengthening or shortening). Rician fading occurs when one of the paths, typically a line of sight signal, is much stronger than the others. In Rician fading, the amplitude gain is characterized by a Rician distribution.

Rayleigh fading is the specialized model for stochastic fading when there is no line of sight signal, and is sometimes considered as a special case of the more generalized concept of Rician fading. In Rayleigh fading, the amplitude gain is characterized by a Rayleigh distribution [16].

1. Motion of people inside building causes Ricean Fading for the stationary receivers.
2. Portable receivers experience in general:
   - Rayleigh fading for OBS propagation paths
   - Ricean fading for LOS paths.

6.2. MULTIPATH DELAY SPREAD

Because of multipath reflections, the channel impulse response of a wireless channel looks likes a series of pulses. In practice the number of pulses that can be distinguished is very large, and depends on the time resolution of the communication or measurement system.

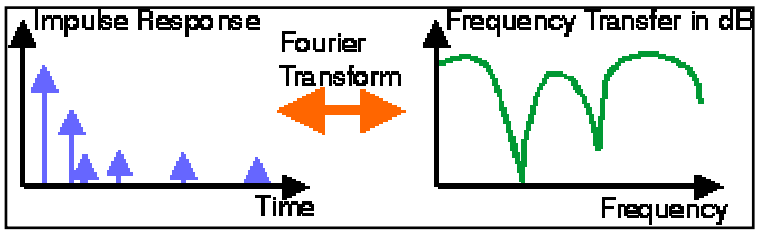

Figure 6.1. Example of impulse response and frequency transfer function of a multipath channel [17]

- The maximum delay time spread is the total time interval during which reflections with significant energy arrives.
- The r.m.s. delay spread T_{RMS} is the standard deviation (or root-mean-square) value of the delay of reflections, weighted proportional to the energy in the reflected waves [17].

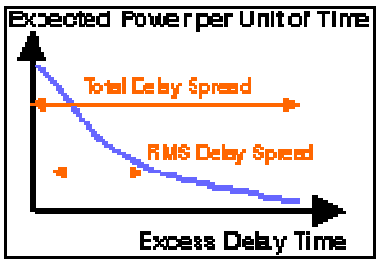

Figure 6.2. Definitions of total delay spread and RMS delay spread [17]

6.2.1 Delay Profile

The delay profile is the expected power per unit of time received with a certain excess delay. It is obtained by averaging a large set of impulse responses.

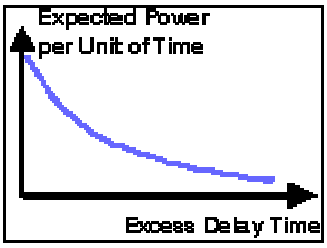

Figure 6.3. Typical delay profile [17]

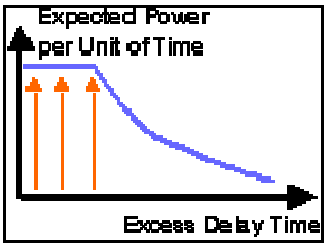

Figure 6.4. Typical indoor delay profile [17]

- Buildings with fewer metals and hard-partitions typically have small rms delay spreads: 30-60ns.

  Can support data rates excess of several Mbps without equalization

- Larger buildings with great amount of metal and open aisles may have rms delay spreads as large as 300ns.

  Cannot support data rates more than a few hundred Kbps without equalization [17].

6.3. PATH LOSS

Path loss (or path attenuation) is the reduction in power density (attenuation) of an electromagnetic wave as it propagates through space. Path loss is a major component in the analysis and design of the link budget of a telecommunication system.

This term is commonly used in wireless communications and signal propagation. Path loss may be due to many effects, such as free-space loss, refraction, diffraction,

reflection, aperture-medium coupling loss, and absorption. Path loss is also influenced by terrain contours, environment (urban or rural, vegetation and foliage), propagation medium (dry or moist air), the distance between the transmitter and the receiver, and the height and location of antennas.

Path loss normally includes propagation losses caused by the natural expansion of the radio wave front in free space (which usually takes the shape of an ever-increasing sphere), absorption losses (sometimes called penetration losses), when the signal passes through media not transparent to electromagnetic waves, diffraction losses when part of the radio wave front is obstructed by an opaque obstacle, and losses caused by other phenomena.

The signal radiated by a transmitter may also travel along many and different paths to a receiver simultaneously; this effect is called multipath. Multipath can either increase or decrease received signal strength, depending on whether the individual multipath wave fronts interfere constructively or destructively. The total power of interfering waves in a Rayleigh fading scenario vary quickly as a function of space (which is known as small scale fading), resulting in fast fades which are very sensitive to receiver position [9].

The following formula that we have seen earlier also describes the indoor path loss:

$$PL(d)[dBm] = PL(d_0) + 10n\log(d/d_0) + Xs \tag{6.1}$$

- n and s depend on the type of the building
- Smaller value for s indicates the accuracy of the path loss model.

Table 6.1. Path loss exponent and standard deviation measured for different buildings [9]

Building	Frequency (MHz)	n	σ (dB)
Retail stores	914	2.2	8.7
Grocery store	914	1.8	5.2
Office, hard partition	1500	3.0	7.0
Office, soft partition	900	2.4	9.6
Office, soft partition	1900	2.5	14.1
Factory LOS			
Textile / Chemical	1300	2.0	3.0
Textile / Chemical	4000	2.1	7.0
Paper / Cereals	1300	1.8	6.0
Metalworking	1300	1.6	5.8
Suburban Home			
Indoor Street	900	3.0	7.0
Factory OBS			
Textile / Chemical	4000	2.1	9.7
Metalworking	1300	3.3	6.8

6.3.1. In Building Path Loss Factors

6.3.1.1. Partition Losses (same floor)

Buildings have a wide variety of partitions and obstacles which from the internal and external structure. Houses typically use a wood frame partition with plaster board to form internal walls and have wood or nonreinforced concrete between floors. Office buildings, on the other hand, often have large open areas which are constructed by using movable office partitions so that the space may be reconfigurated easily, and use metal reinforced concrete between floors. Partitions that are formed as part of the building structure are called hard partitions, and partitions that may be moved and which do not span to the ceiling are called soft partitions. Partitions vary widely in their physical and electrical characteristics, making it difficult to apply general models to specific indoor installations. Nevertheless, researchers have formed extensive data bases of losses for a great number of partitions [9].

There are two kind of partition at the same floor:

- Hard partions: the walls of the rooms
- Soft partitions: moveable partitions that does not span to the ceiling

The path loss depends on the type of the partitions.

Table 6.2. Average signal loss measurements reported by various researches for radio paths obstructed by some common building material [9]

Material Type	Loss (dB)	Frequency (MHz)
All metal	26	815
Aluminum siding	20.4	815
Concrete block wall	3.9	1300
Loss from one floor	20-30	1300
Turning an angle in a corridor	10-15	1300
Concrete floor	10	1300
Dry plywood (3/4in) – 1 sheet	1	9600
Wet plywood (3/4in) – 1 sheet	19	9600
Aluminum (1/8in) – 1 sheet	47	9600

6.3.1.2. Partition Losses Between Floors

The losses between floors of a building are determined by the external dimensions and materials of the building, as well as the type of construction used to create the floors and the external surroundings. Even the number of the Windows in a building and the presence of tinting (which attenuates radio energy) can impact the loss between floors [9].

The losses between floors of a building are determined by

- External dimensions and materials of the building
- Type of construction used to create floors
- External surroundings
- Number of windows

- Presence of tinting on windows

Table 6.3. Average floor attenuation factor in dB for one, two, three and four floors in two office buildings [9]

Building	FAF (dB)	σ (dB)
Office building 1		
Through 1 floor	12.9	7.0
Through 2 floors	18.7	2.8
Through 3 floors	24.4	1.7
Through 4 floors	27.0	1.5
Office building 2		
Through 1 floor	16.2	2.9
Through 2 floors	27.5	5.4
Through 3 floors	31.6	7.2

6.3.1.3. Signal Penetration into Buildings

Quality of radio signals of such cellular system especially indoor coverage is the major limiting factor to maintain and improve their quality of services. Indoor coverage can be built by using power splitters to deliver signal from the outdoor antenna to indoor antenna distribution system. The propagation of radio signal through buildings is strongly influenced by the building layout, the construction materials and the building type. Walls and obstacles made of different materials obstruct the signal differently. It is found that the wall penetration for 900 MHz signals can be in the range of 15 to 27dB, depending on the building construction. The building penetration in the window area is approximately 6dB [18].

As the equation below γ is penetration (skin depth), ω is angular frequency, μ is permeability, ε is permittivity.

$$\gamma = \sqrt{j\,\omega\mu\,(\sigma + j\,\omega\varepsilon)} = j\,\beta_0 N \tag{6.2}$$

Where N is the refraction index,

$$N = \sqrt{\varepsilon_r - j\frac{\sigma}{\omega\,\varepsilon_0}} \tag{6.3}$$

- RF signals can penetrate from outside transmitter to the inside of buildings
  - However the signals are attenuated
- The path loss during penetration has been found to be a function of:
  - Frequency of the signal
  - The height of the building

  - Effect of Frequency
    - Penetration loss decreases with increasing frequency
  - Effect of Height
    - Penetration loss decreases with the height of the building up-to some certain height
      - At lower heights, the urban clutter induces greater attenuation
    - and then it increases
      - Shadowing affects of adjacent buildings

7. INDOOR PROPAGATION MODELS

Indoor propagation is the one of the most important problem for nowadays. Increasing the demand of mobile technology GSM, WLAN and 3G causes so many problems. Therefore there exists to solve these problems some indoor models [9].

- Long Distance Path Loss Model
- Erickson Multiple Breakpoint Model
- Attenuation Factor Model
- Ray Tracing Model

8. DEFINITION OF THE MODEL

Our office model is constructed by the electromagnetic modelling techniques and five times smaller than the real office room. Also furnitures are made five times smaller than the real office furnitures. Office model's walls, ceiling and floor is composed of three layered materials. First layer (interior) is made of wood. Second layer is made of ceramic. Third layer (outer) is made of wood. There is wide window which is made of wooden sticks and covered with aluminum foil. Floor part was made ceramic material. For the measurements there exists a ladder and on the ladder there is a sliding way. Model's outer side covered by the absorber as the Figure 8.1 (made of special material and absorbs electromagnetic waves).

I assume that an office room's wall height is 3 meters, and at indoor applications base stations must be located 15 cm down from the ceiling at the wall. For my project I locate transmitter antenna above 57 cm from the floor. Receiver antenna height changes from a person, who is 170 cm height. Therefore there are two situations for the measurements. First situation is when a person is sitting on a chair; height is equal to 60 cm. In order to the electromagnetic theory principles; I applicate this to my project the height changes 18 cm. Second situation is when a person stands up; height is equal to 1.70 cm. When I applicate this to my project the height changes 34 cm. Only the receiver antenna height change. Every measurement made by two polarizations (TE and TM modes).

Our operation frequency is 9.4 GHz. Also I have to cover the horn antenna's body with the absorber but we do not have small size absorber for that size, therefore we will see the how that area affects the propagation at the results part.

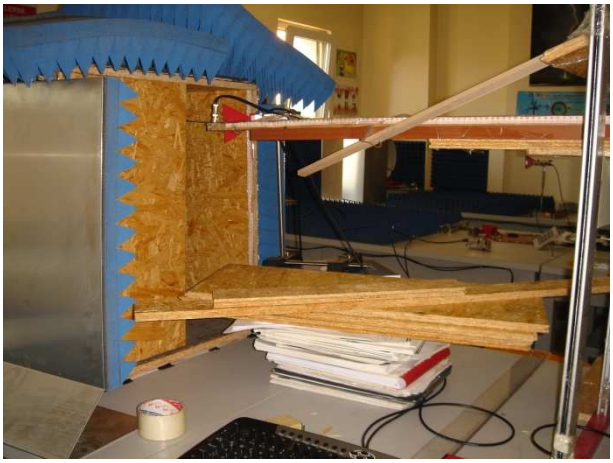

Figure 8.1. Front side of the model and measurement ladder and sliding way

Measurement ladder must be made of wooden material in order not to affect propagation. Wooden material requires construction knowledge and practical knowledge. Therefore measurement ladder made of metal material; but it affects measurement's results. Metallic surfaces increase propagation; therefore I cover it by the absorber as the Figure 8.2.

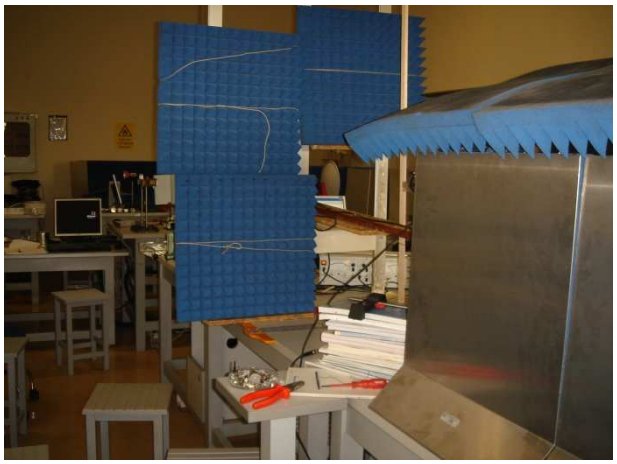

Figure 8.2. Measurement ladder and sliding way

Figure 8.3. Model's window

Figure 8.4. Model's measurement hole, Tx and Rx antennas

Interior part of the model is composed of cartoon office furniture. This material is used because its dielectric properties are similar with the woods, and also making small furniture easier than wood.

There is three type of measurement scenario.

First scenario is free office room measurements. For the free office room measurements interior side of the office is free (there is no furniture or human).

Figure 8.5. Free office room

Second scenario is all the office furnitures are arranged like a real office room. Furnitures are made of cartoon. Water bottles represents person in the office room. Water bottles were filled with the mixture of sea water and drinking water (1/4), to have same dielectric properties with the human being.

Figure 8.6. Interior side of the cartoon furnitured office room model

Figure 8.7. Interior side of the cartoon furnitured office room model

Third scenario is all the office furnitures are arranged like a real office room. Furniture are made of cartoon and covered with by aluminum foil. Aluminum foil is used for to increase scattering and reflection. Water bottles represents person in the office. Water bottles were filled with the mixture of sea water and drinking water (1/4), to have same dielectric properties with the human being.

Figure 8.8. Interior side of the metallic furnitured office room model (all cartoon furniture covered with aluminum foil)

Figure 8.9. Interior side of the metallic furnitured office room model (all cartoon furniture covered with aluminum foil)

Figure 8.10. Interior side of the metallic furnitured office room model (all cartoon furniture covered with aluminum foil)

8.1. MEASUREMENT RESULTS OF THE MODEL

8.1.1. Free Office Measurements

First scenario is at the free office room. The height of the receiver antenna is 18, 34 cm and the height of the transmitter antenna is 57 cm. There is no furniture or office material located.

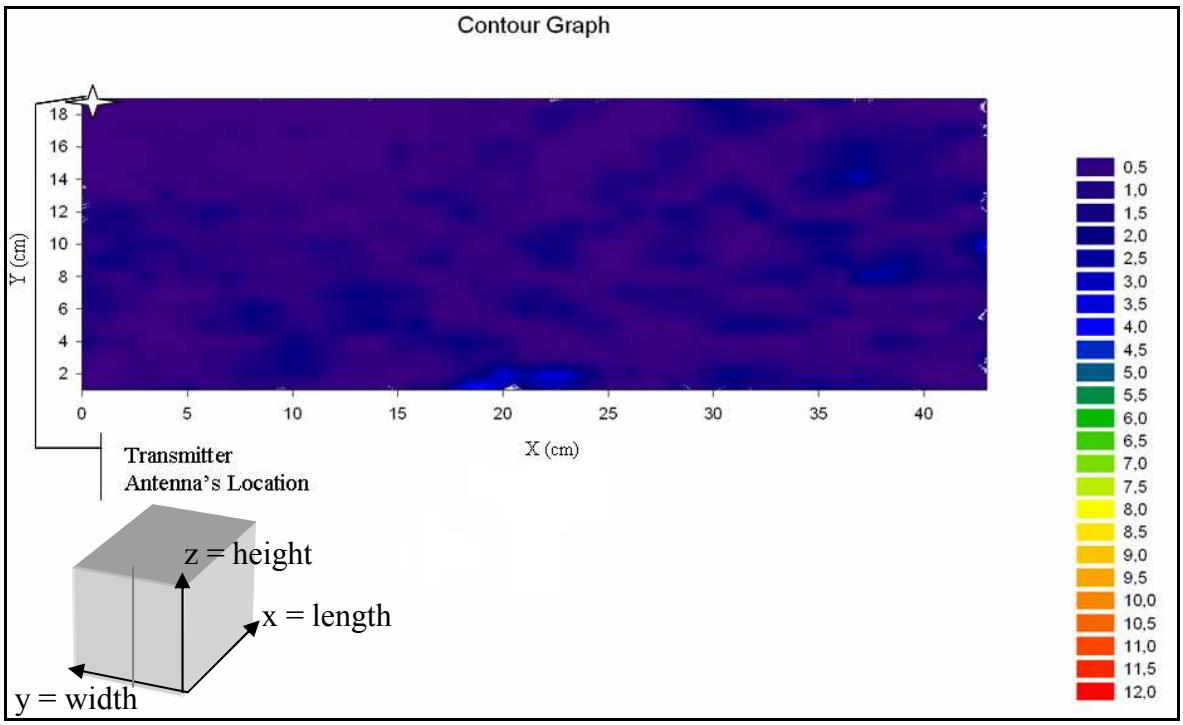

Figure 8.11. Free room receiver antenna height 18 cm TE polarization

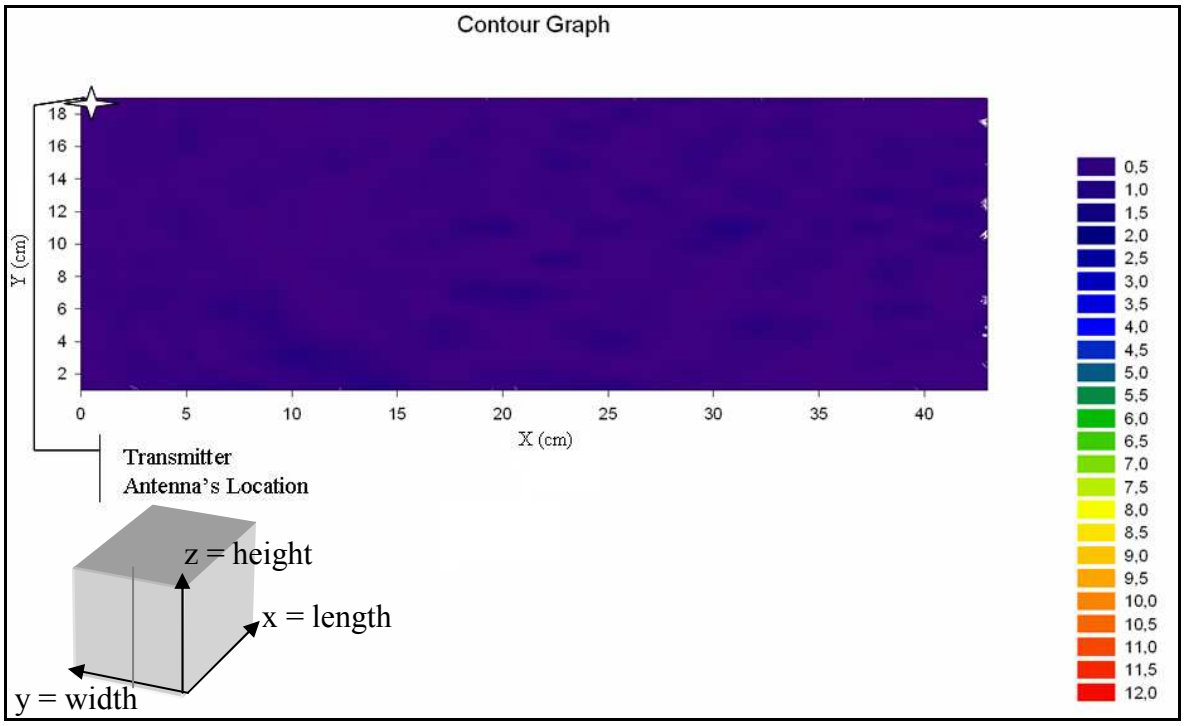

Figure 8.12. Free room receiver antenna height 18 cm TM polarization

From the Figures 8.11 and 8.12, it can be seen that there is homogeneous electric field distribution inside the room, because there is no scattering objects in the room.

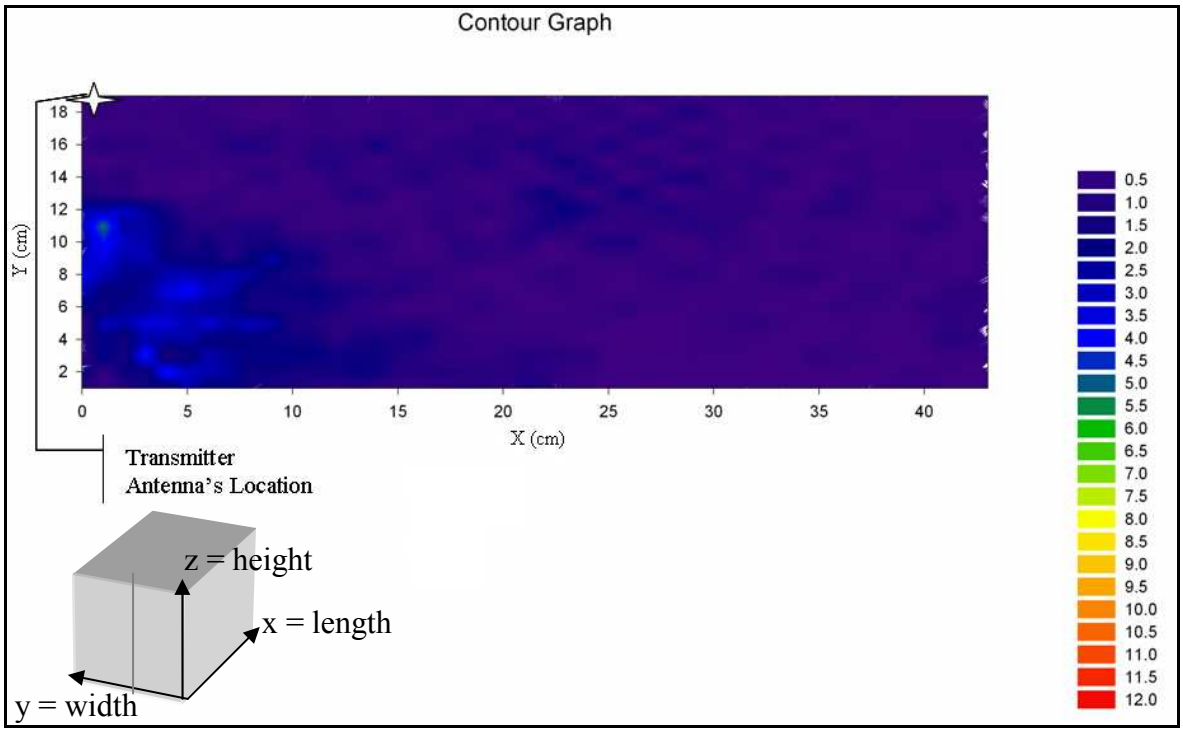

Figure 8.13. Free room receiver antenna height 34 cm TE polarization.

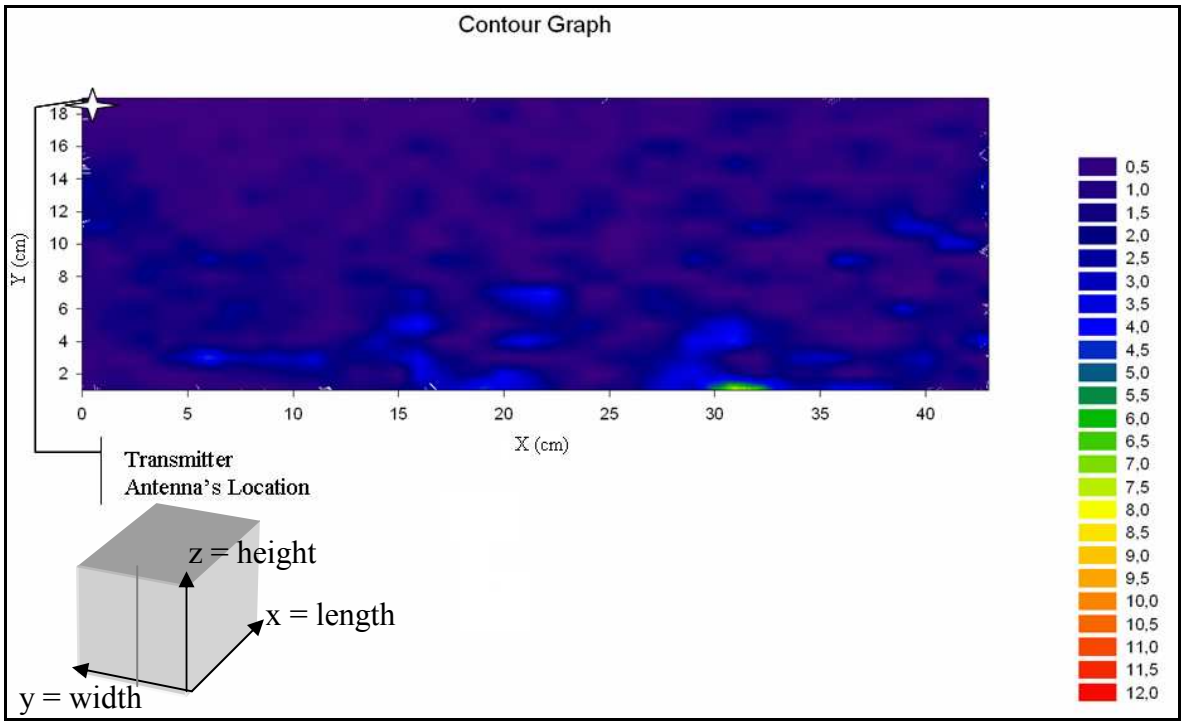

Figure 8.14. Free room receiver antenna height 34 cm TM polarization.

From the Figures 8.13 and 8.14, the homogeneous electric field distribution changes inside the room, it is because of that the receiver antenna is close to the transmitter antenna at that measurement height.

8.1.2. Cartoon Furniture Office Measurements

Second scenario is at the cartoon furnitured office room. The height of the receiver antenna is 18, 34 cm and the height of the transmitter antenna is 57 cm.

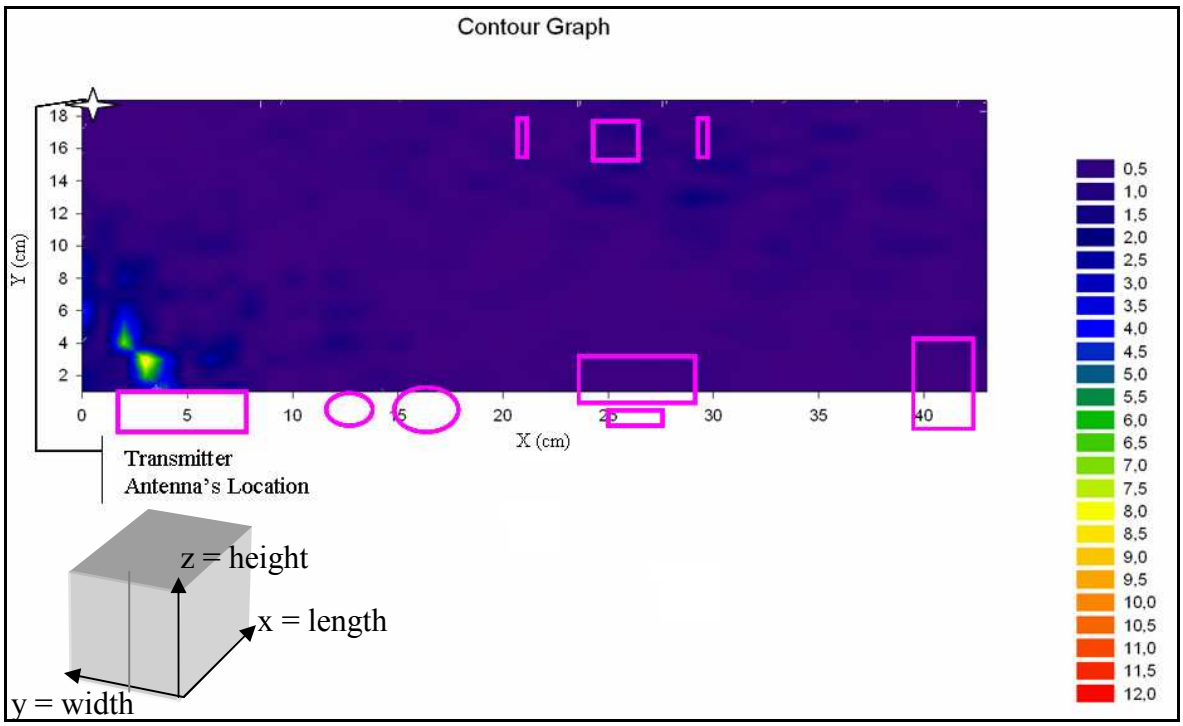

Figure 8.15. Cartoon furniture room receiver antenna height 18 cm TE polarization

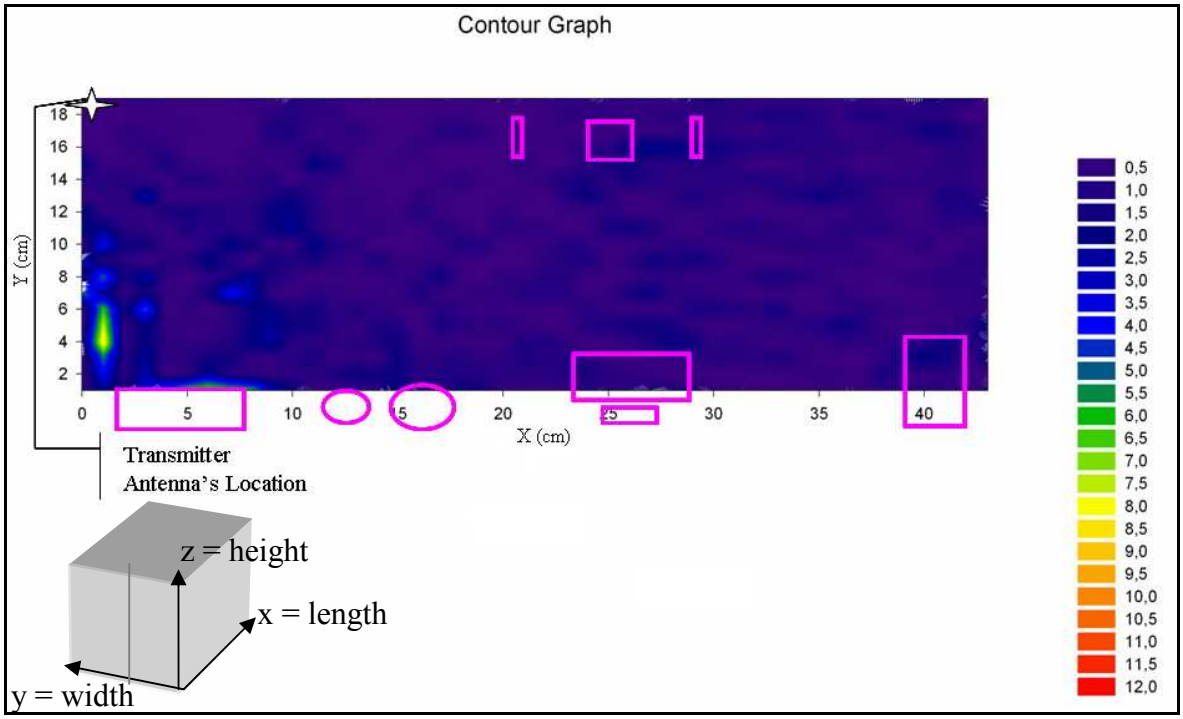

Figure 8.16. Cartoon furniture room receiver antenna height 18 cm TM polarization

From the Figures 8.15 and 8.16, there is color changes which show the propagation mechanisms (reflection, refraction and scattering). Cartoon furniture behaves like an absorber. Therefore there is nearly homogeneous electric field distribution. Also from the figures, at the left hand side there is more densely changes. It is because of that the cupboards handle which are made of metallic screws. The difference between the TE and TM polarizations is that, at TE polarization wave propagates horizontally and the position of the screws are also horizontal. But at the TM mode, wave propagates vertically.

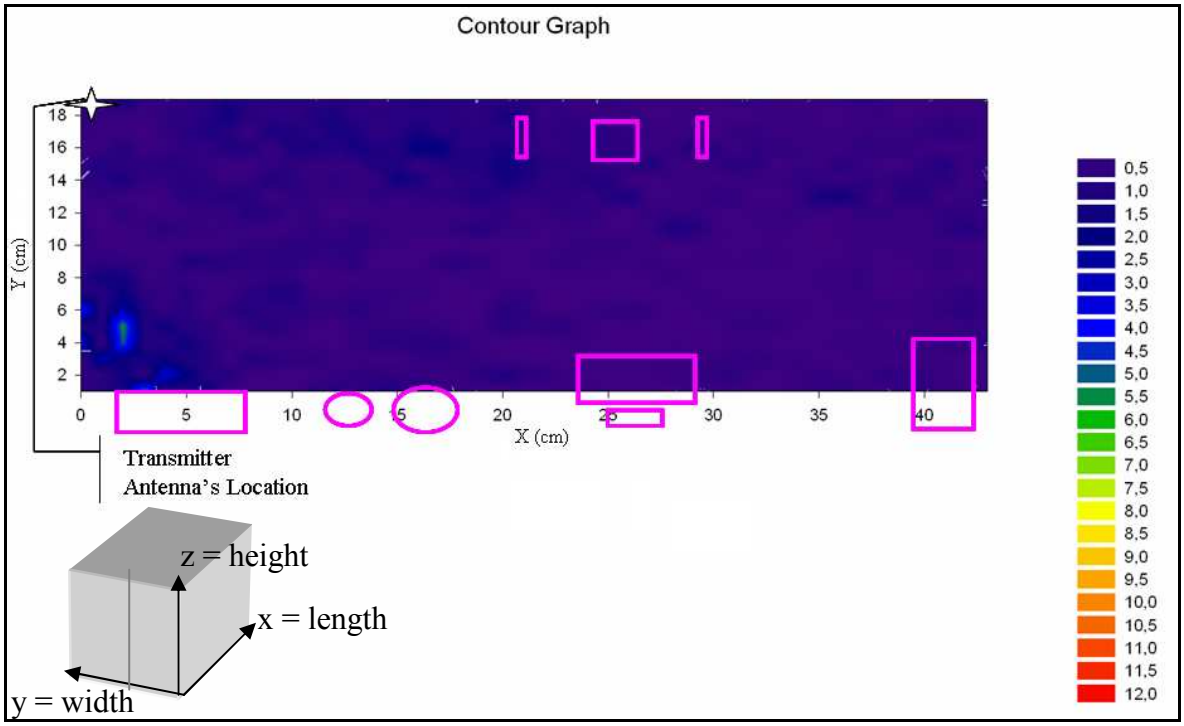

Figure 8.17. Cartoon furniture room receiver antenna height 34 cm TE polarization

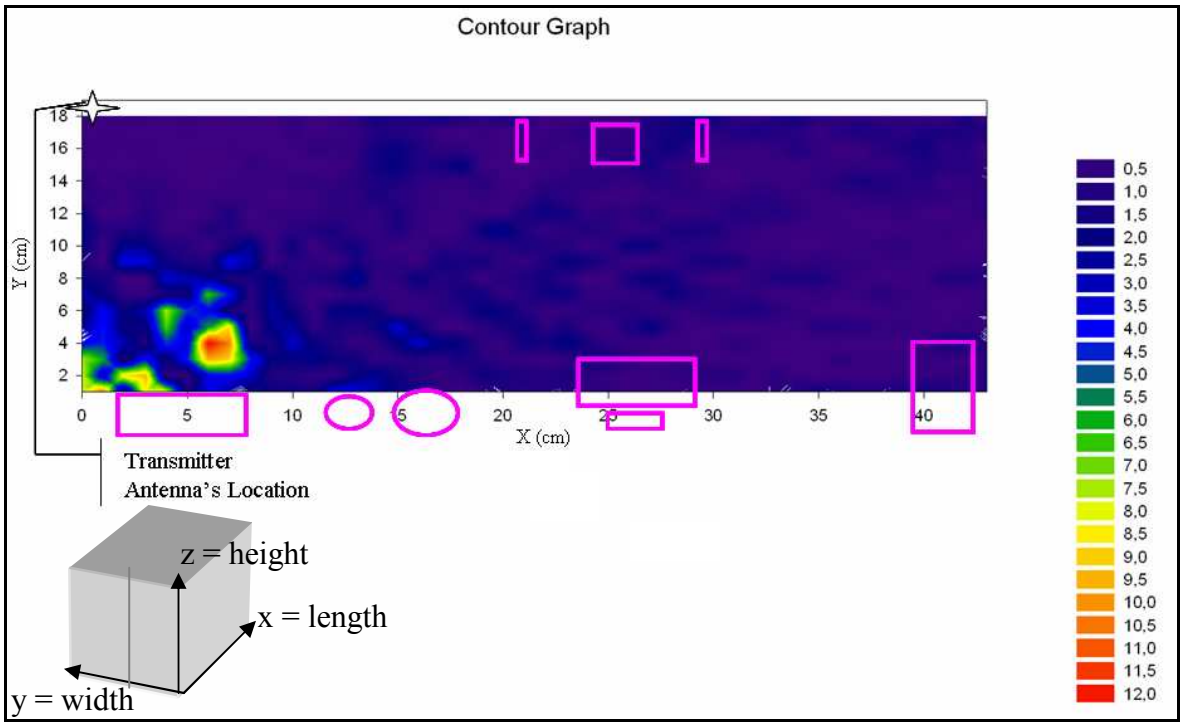

Figure 8.18. Cartoon furniture room receiver antenna height 34 cm TM polarization

From the Figures 8.17 and 8.18, there are changes in electic field distribution, it is because of that the receiver antenna is close to the transmitter antenna. Also from the figures left hand side there is more densely changes. It is because of the cupboards handles which are made of metallic screws.

8.1.3. Metal Furniture Office Measurements

Third scenario is at the furniture (metal) office. The height of the receiver antenna is 18, 34 cm and the height of the transmitter antenna is 57 cm.

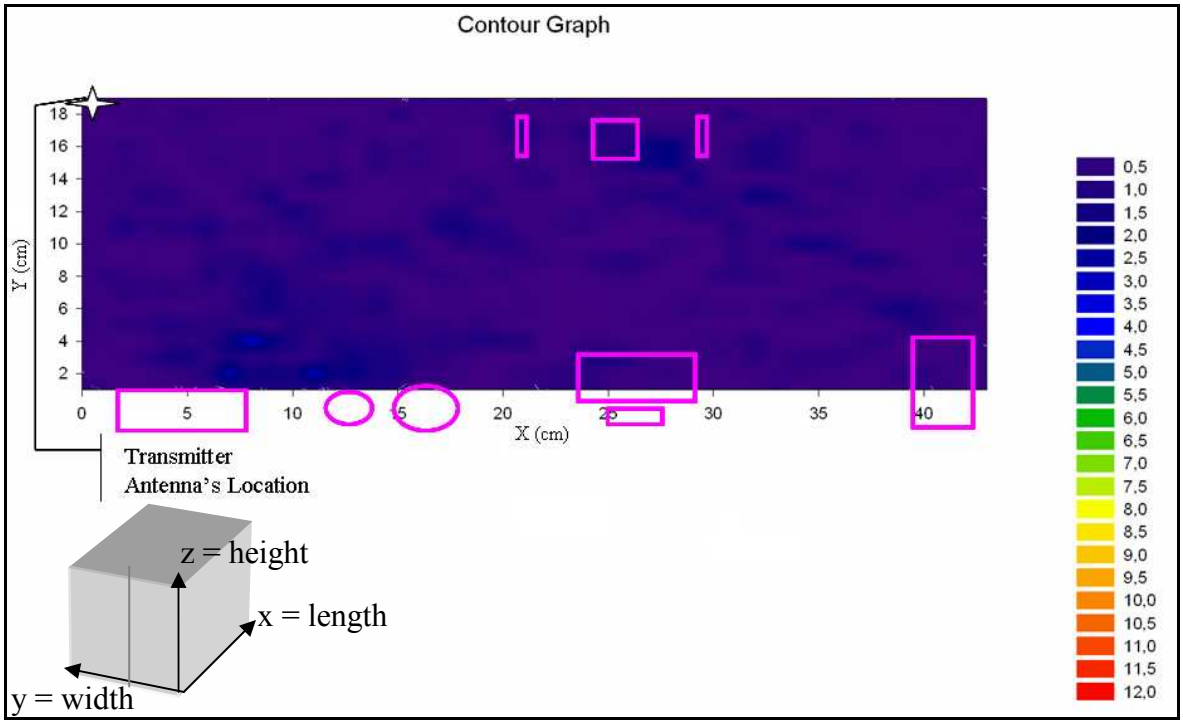

Figure 8.19. Metal furniture room receiver antenna height 18 cm TE polarization

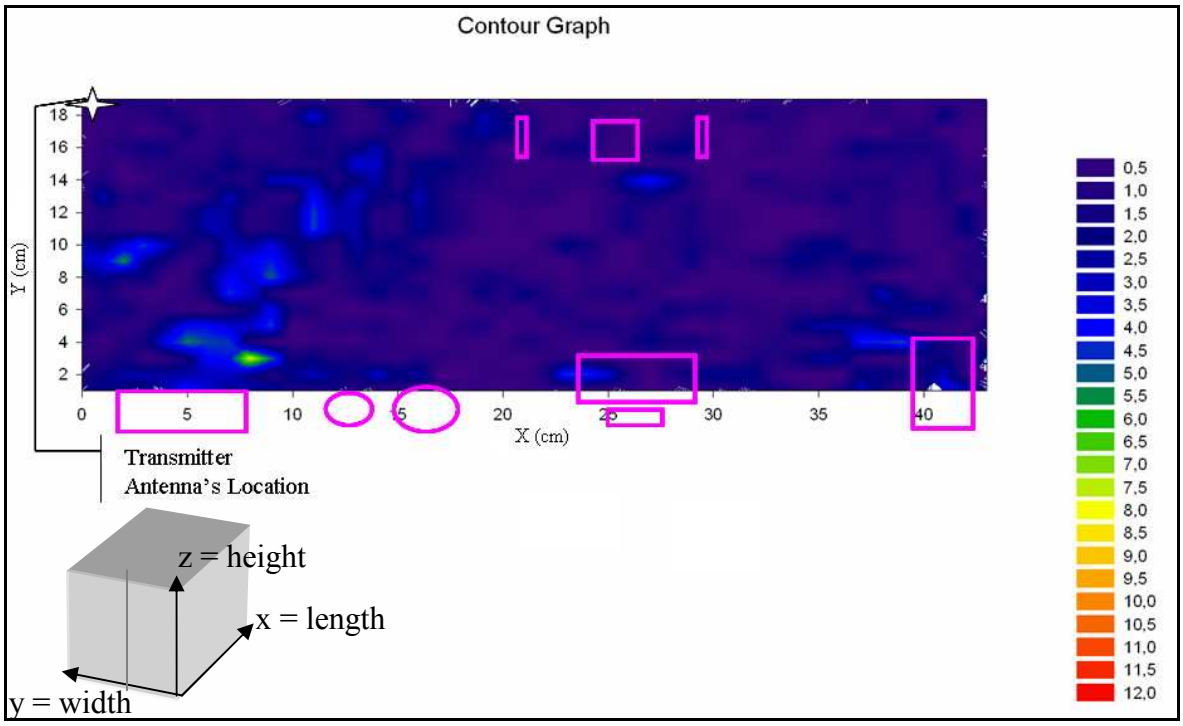

Figure 8.20. Metal furniture room receiver antenna height 18 cm TM polarization

From the Figures 8.19 and 8.20, color changes show the propagation mechanisms (reflection, refraction and scattering). When I put the aluminum foil covered cartoon furniture, heterogeneous electric field distribution occured. Unlike the TE polarization, at TM polarization electric field intensity increased. Because all the furnitures are located vertically and waves propagates vertically at TM polarization.

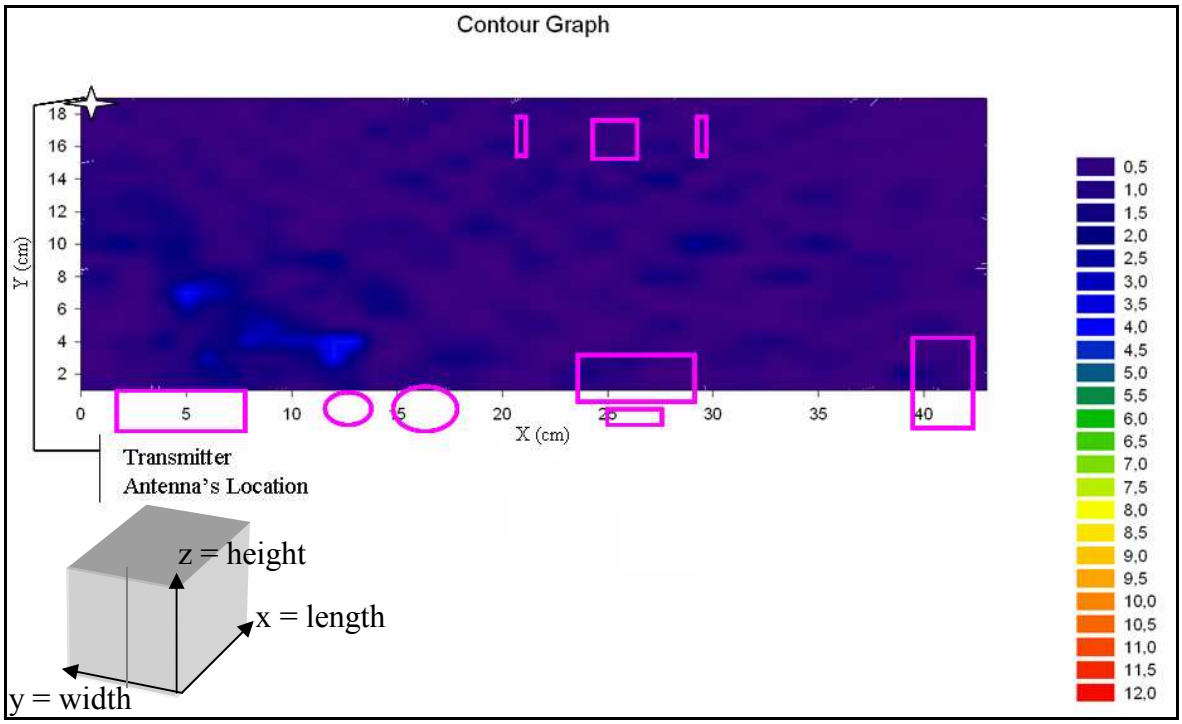

Figure 8.21. Metal furniture room receiver antenna height 34 cm TE polarization

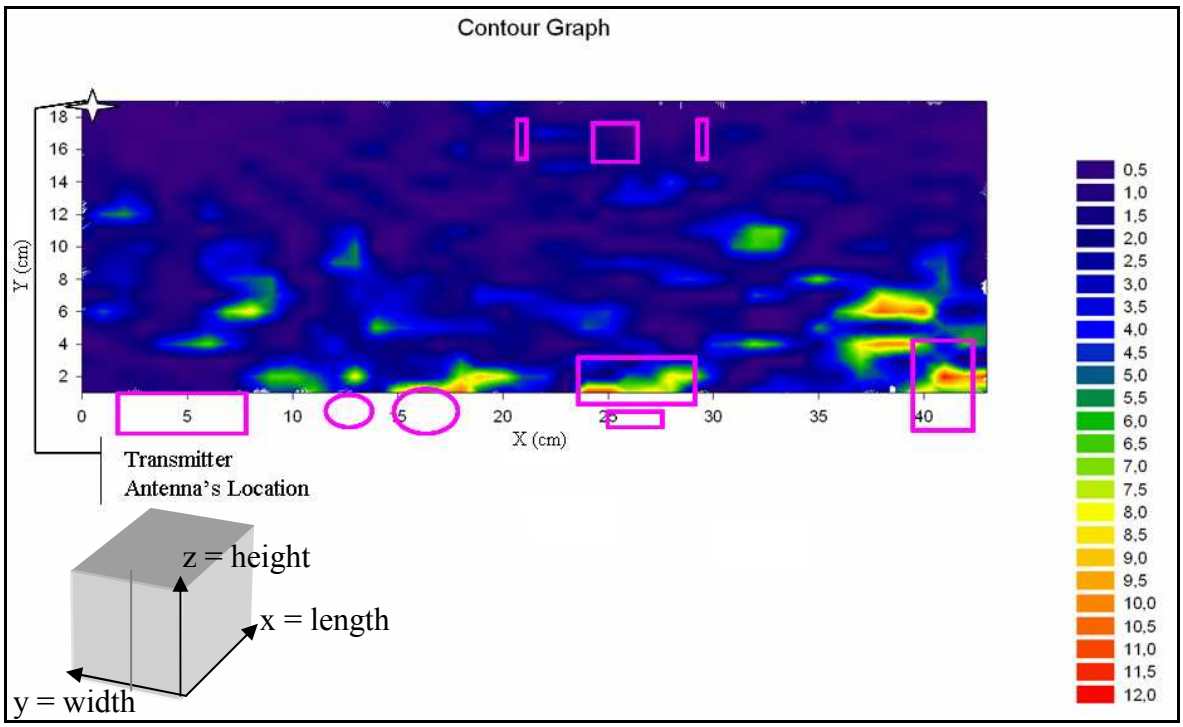

Figure 8.22. Metal furniture room receiver antenna height 34 cm TM polarization

From the Figures 8.21 and 8.22, color changes show the propagation mechanisms (reflection, refraction and scattering). Floor surface is ceramic. When I put the aluminum foil covered cartoon furniture, electric field intensity increased. Also electric field distribution changes a lot. It is because of the receiver antenna is close to the transmitter antenna. Unlike the TE polarization, at TM polarization electric field intensity increased. Because all the furnitures located vertically and waves propagates vertically at TM polarization.

9. SIMULATION RESULTS OF FEKO

Model was constructed in the simulation program FEKO like Figures 9.1., 9.2., 9.3., 9.4., 9.5. All the variables are given to the FEKO as like the model. All the scenarios (free office, office filled with cartoon furniture, office filled metal furniture) was modelled in FEKO. Also all of these measurements are made by Transverse Electric (TE) and Transverse Magnetic (TM) modes.

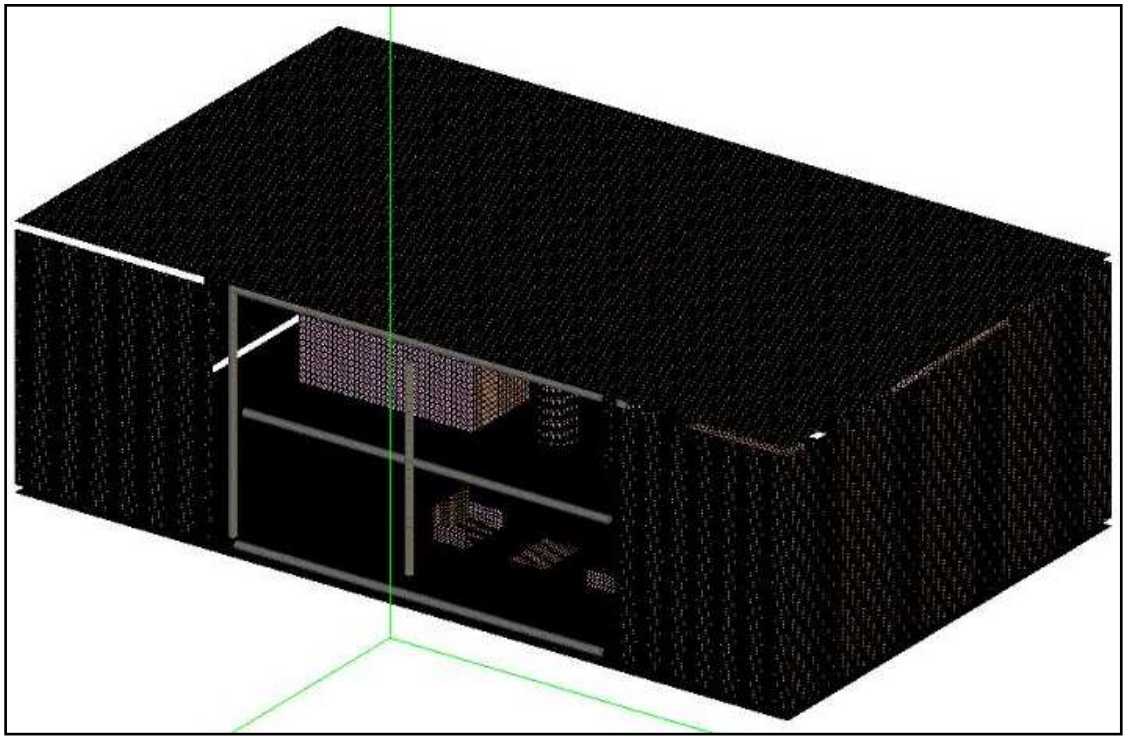

Figure 9.1. Simulation model of FEKO

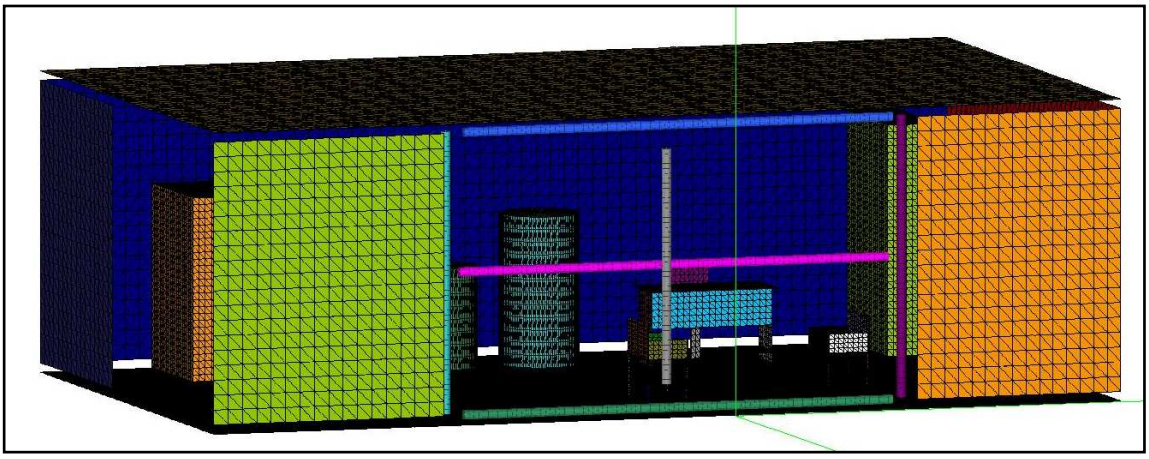

Figure 9.2. Simulation model of FEKO (window side)

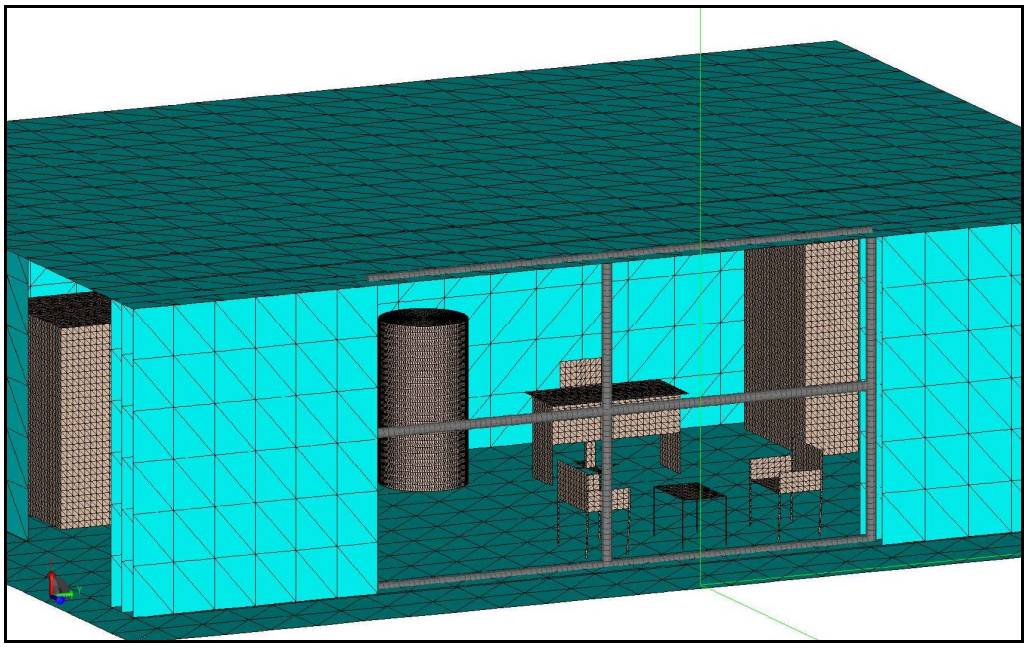

Figure 9.3. Simulation model of FEKO (window side 2)

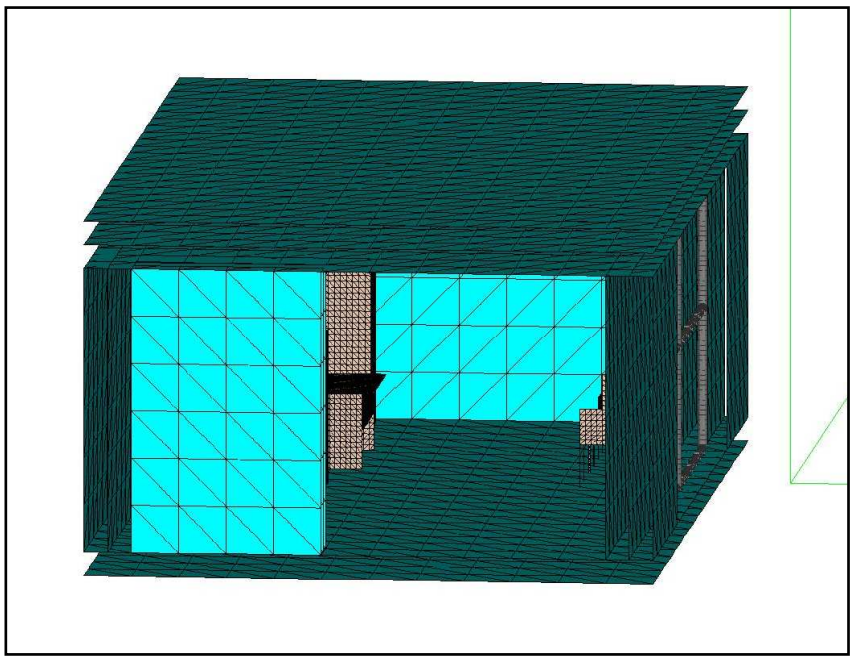

Figure 9.4. Simulation model of FEKO (measurement hole)

The simulations of the model always gave errors because of too many unknowns for mesh elements. The computers used are not enough, it must be equipped with at least much more than 5 TB harddisk and 16 GB RAM. The main reason of “too many unknowns” is that the surface dimensions of the walls are too large compared to the operation wavelength. If we omit the walls and the second scenerio with cartoon furniture room is applied (the height of the receiver antenna is 18, 34 cm and the height of the transmitter antenna is 57 cm), and run the simulation it took 6 days to get the results. The results are shown in Figure 9.6 and Figure 9.7.

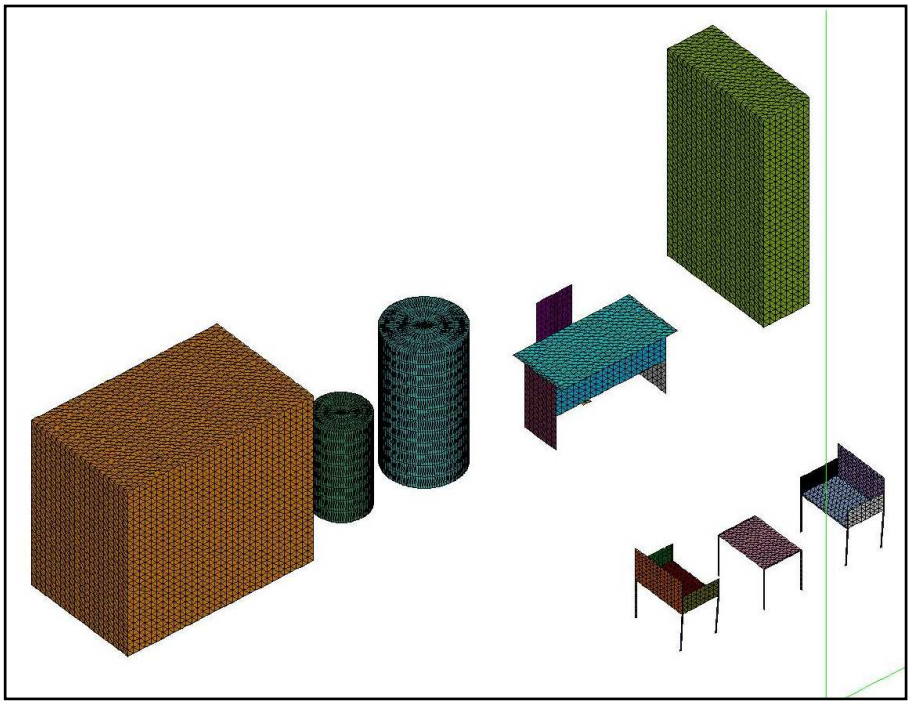

Figure 9.5. Simulation model of FEKO (interior side)

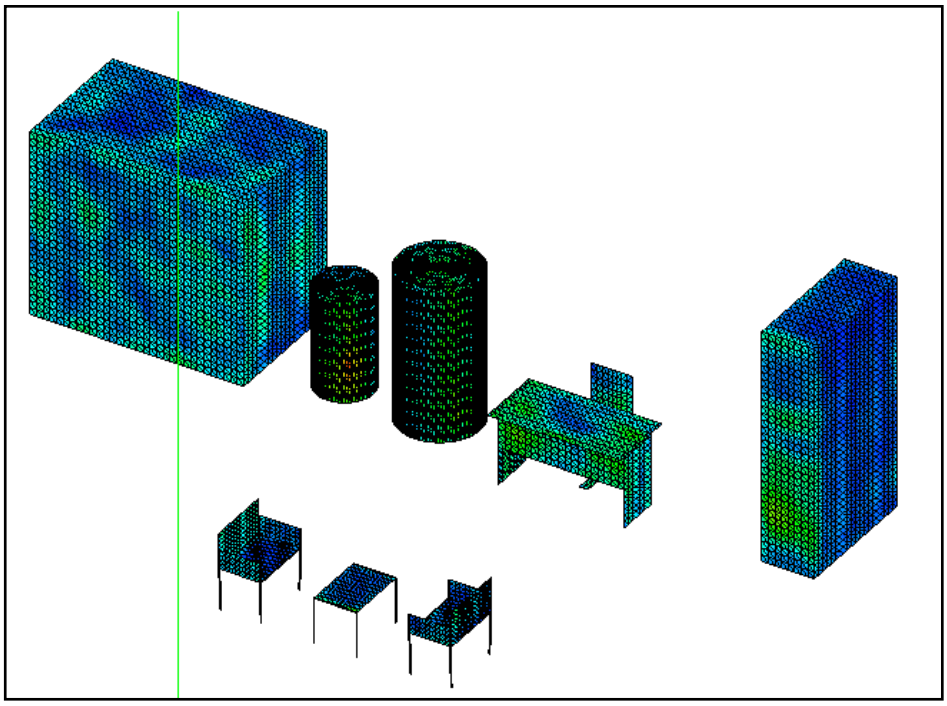

Figure 9.6. Current distribution simulation result of the model without walls

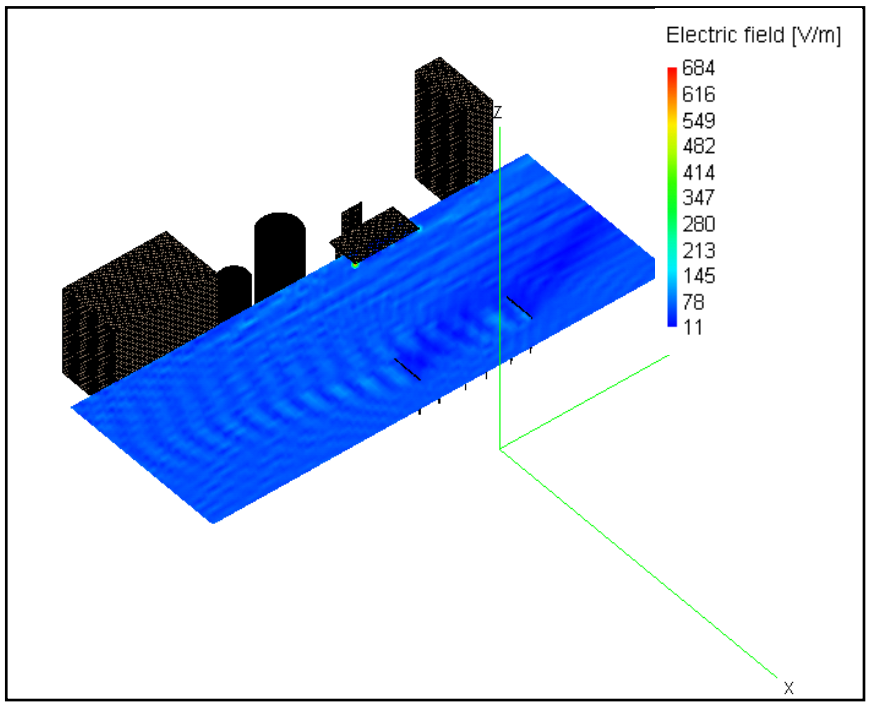

Figure 9.7. Electric field distribution simulation result of the model without walls

In the office rooms there is too many metal objects around. Every metallic objet has scattering property. Some examples for metallic objets in the offices are; cahir legs, radiator pipes, cloth hangs, desk legs and handles etc. If we think that all of these objets as a part of an office room in a composition, it is hard to find electric field distribution by analytically methods. If we work over one by one, it is achievable to explain electric field distribution by analytical methods.

From the figures 9.8 to 9.19 there is electric far field distribution simulation results, for the objects which are used in our office room model. Transmitter antenna is located in same direction and height like the model. Operation frequency is 9.4 GHz. Also objects locations are the same in model.

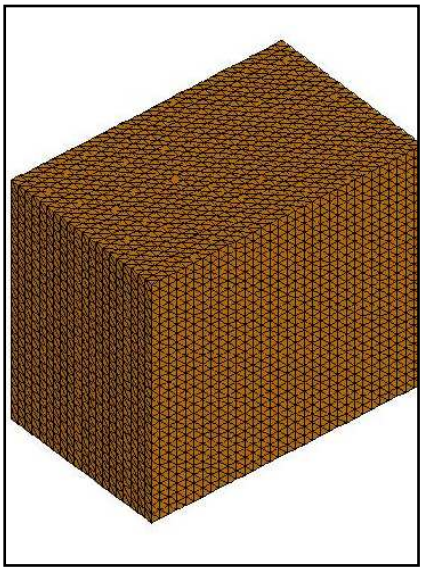

Figure 9.8. Cupboard 1

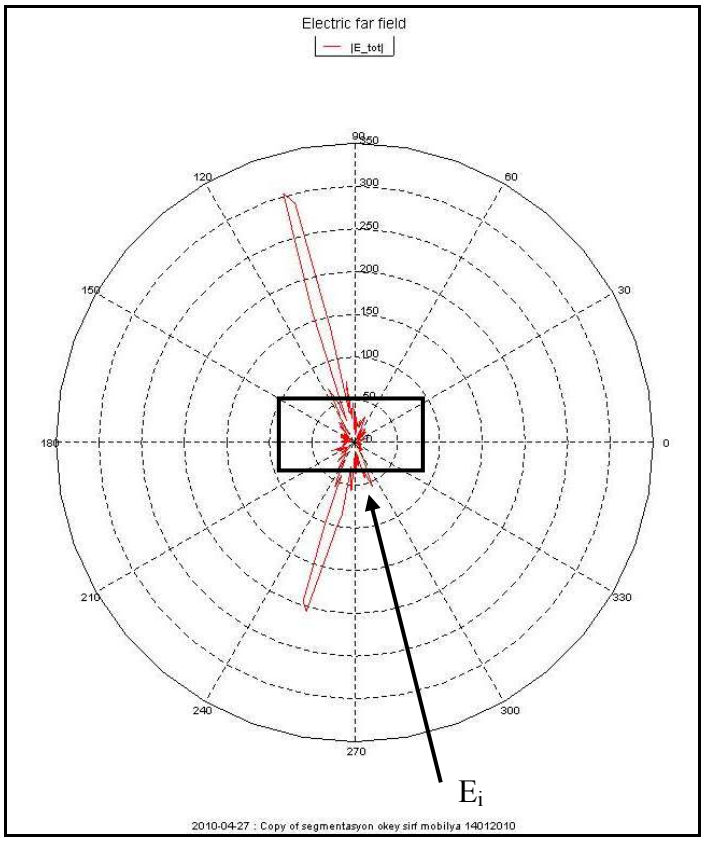

Figure 9.9. Electric far field distribution simulation result of the cupboard 1 without walls

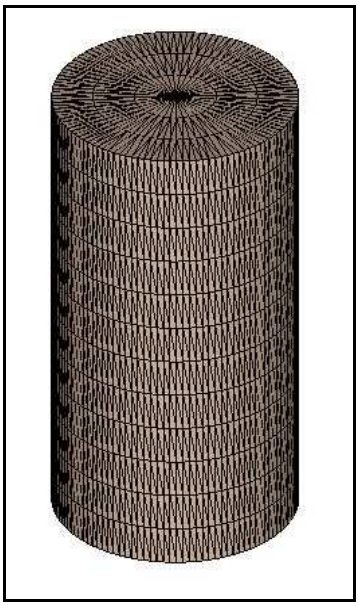

Figure 9.10. Person

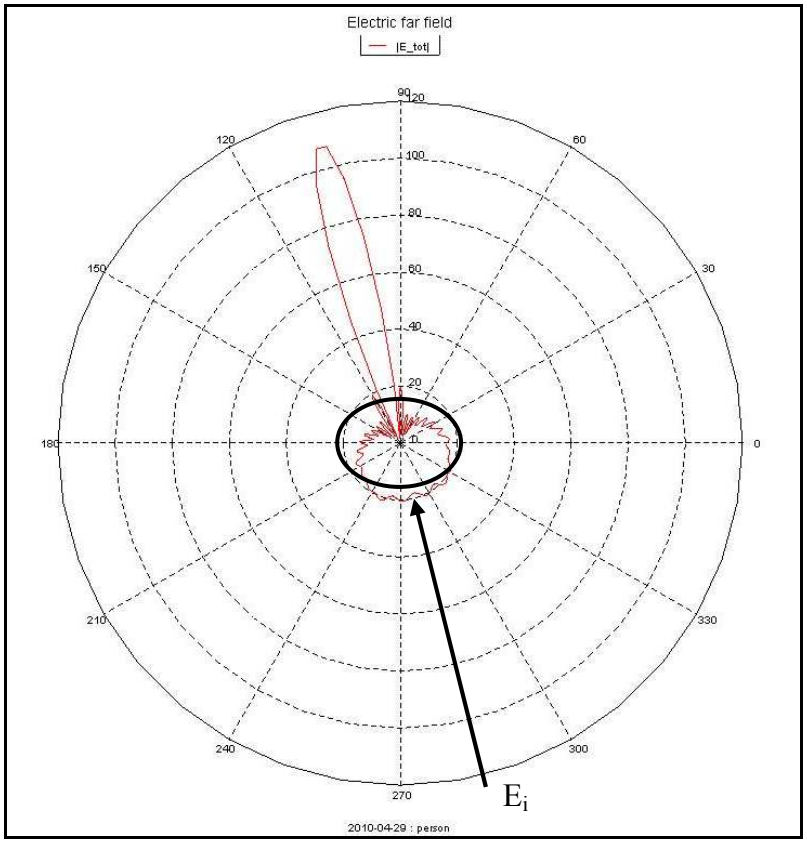

Figure 9.11. Electric far field distribution simulation result of the person without walls

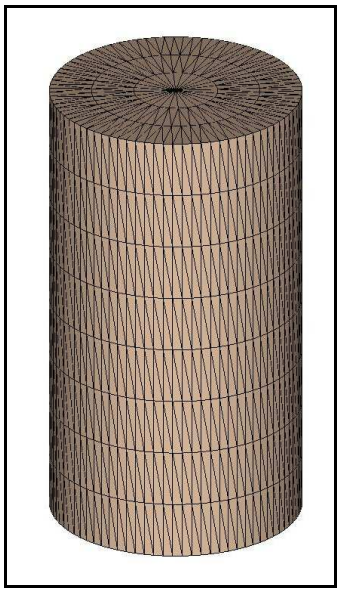

Figure 9.12. Child

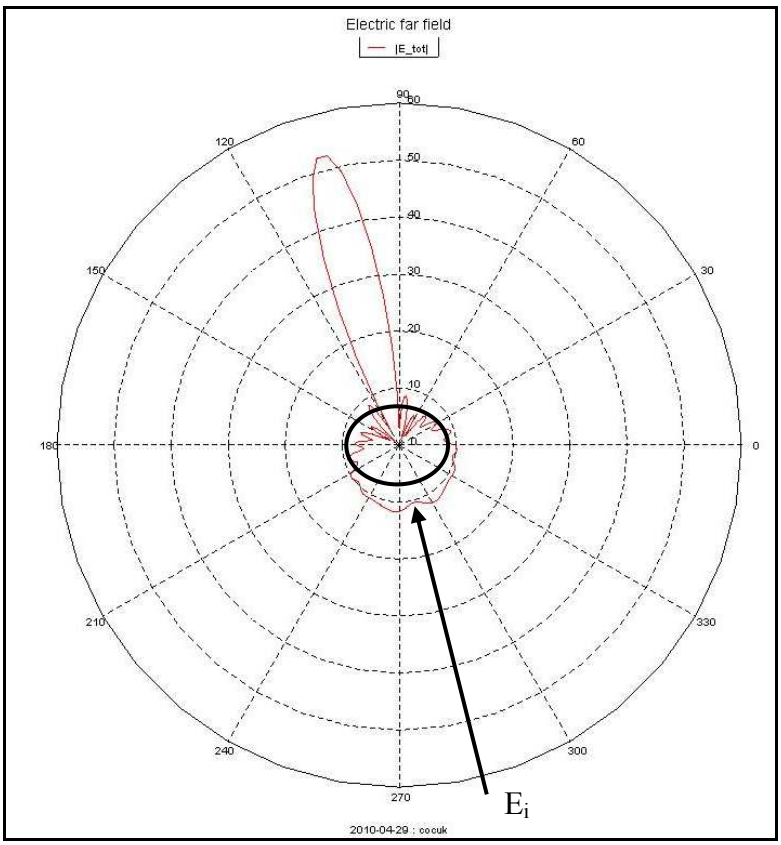

Figure 9.13. Electric far field distribution simulation result of the child without walls

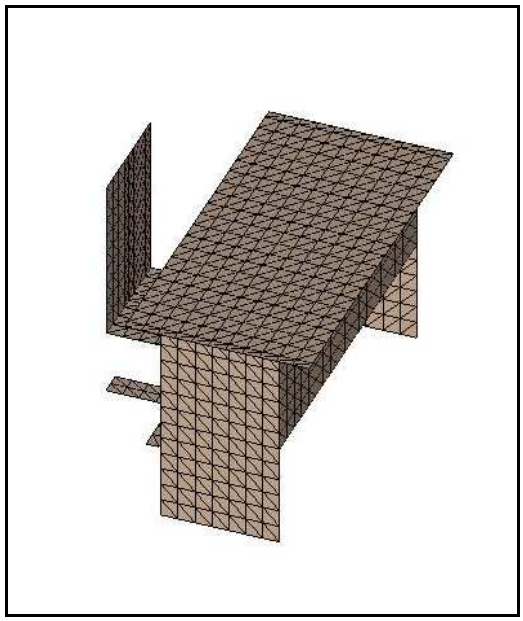

Figure 9.14. Work desk and chair

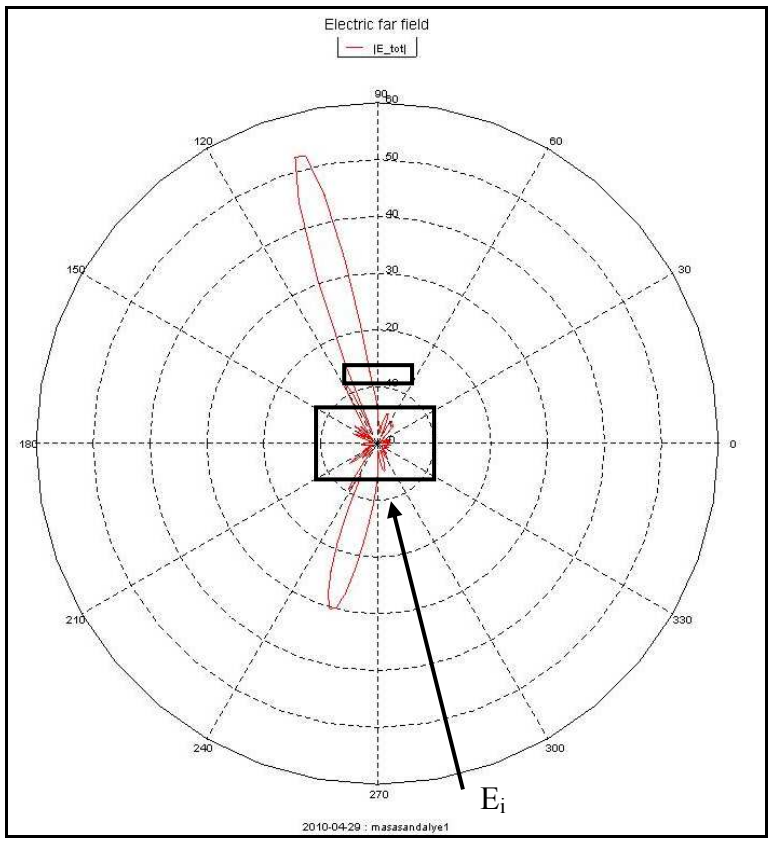

Figure 9.15. Electric far field distribution simulation result of the work desk and chair without walls

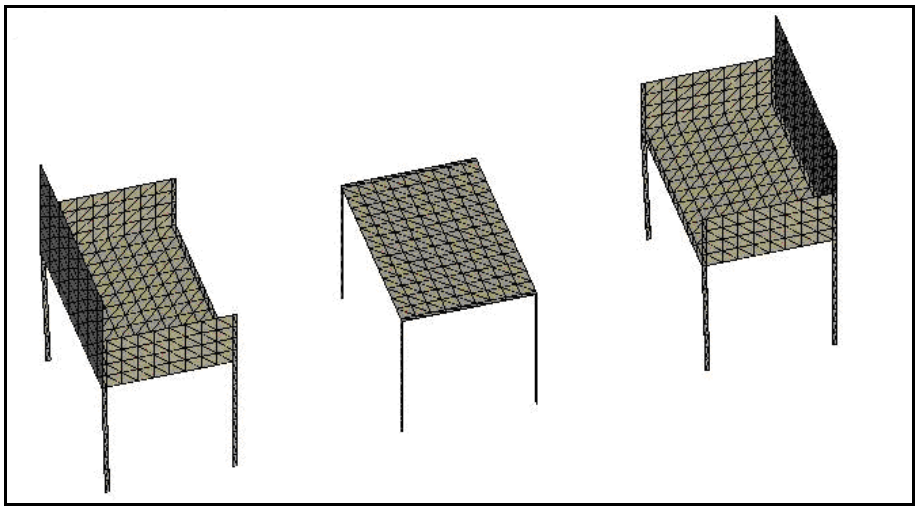

Figure 9.6. Guest table and chairs

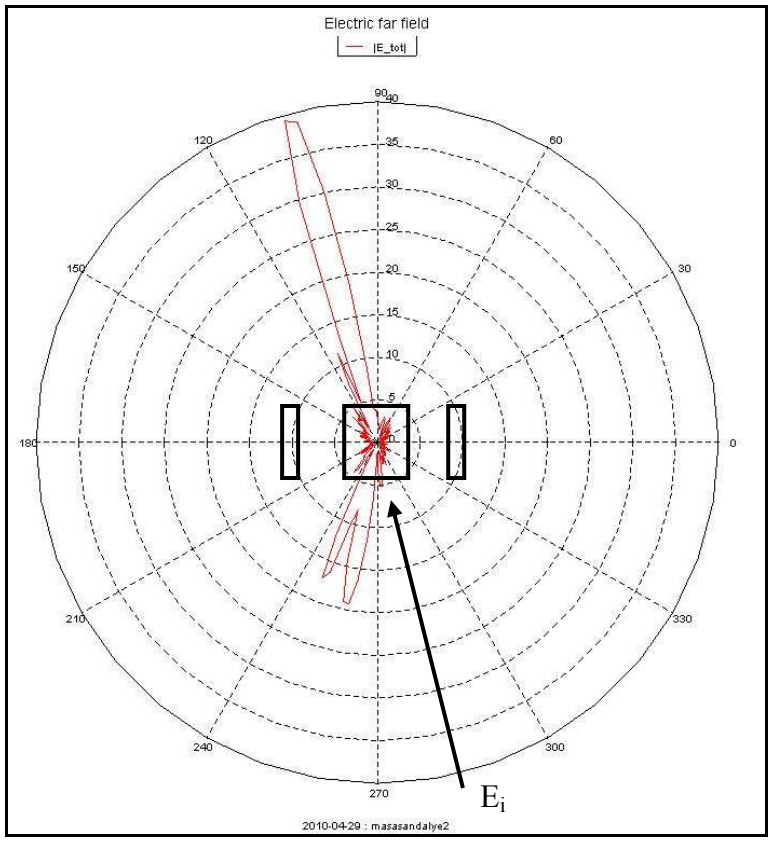

Figure 9.17. Electric far field distribution simulation result of the guest table and chairs without walls

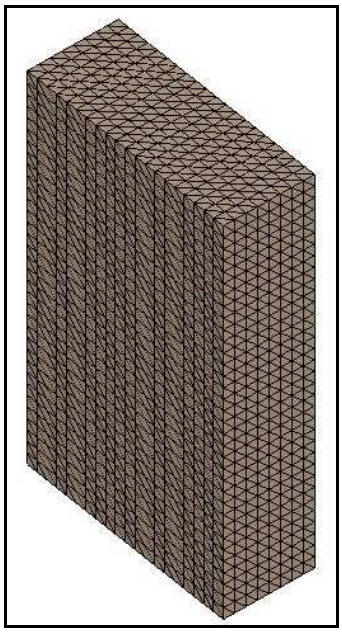

Figure 9.18. Cupboard 2

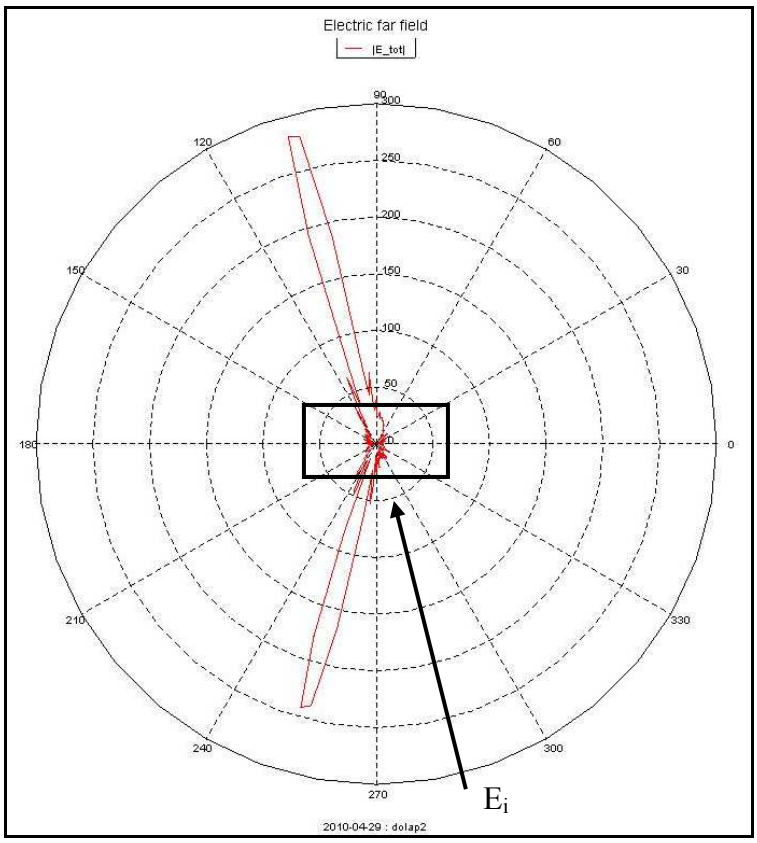

Figure 9.19. Electric far field distribution simulation result of the cupboard 2 without walls

10. CONCLUSION

In this study indoor propagation model was developed for an office room. Three type scenarios were formed to understand indoor propagation mechanisms and the material effects.

It is aimed to compare FEKO simulation program technique with the measurement results of a classical model in a challenging office building environment. Both methods benefited from the use of site-specific measurements. For example, for both measurements and simulations, we have to mesh the measurement surfaces, and for both of them we have to identify the materials. It is observed that metallic objects inside the office room caused the increment of the field intensities. In addition, TM mode polarization is effective more than TE mode polarization inside the room, because most of the objects are aligned vertically inside the room. But for this complicated simulation, the computer used are not enough, it must be equipped with at least much more than 5 TB harddisk and 16 GB RAM.

In the future study, more scenarios must be formed to understand indoor propagation deeply. And also, to get more accurate results for the indoor propagation, rather than using electromagnetic modeling techniques, field distributions should be measured in real office rooms at the real operation frequencies.

APPENDIX A: DIELECTRIC PROPERTIES OF MATERIALS

Table A.1. Solids

Material	Temparature (°C)	Frequency	Relative Permittivity (εr')	Conductivity (σ)
Cellulose (see also paper)				
Cellophane	20	50 Hz/1 MHz	7.6/6.7	100/650
Paper fibres	20	50 Hz	6,5	50
Ceramics				
Alumina	20/100	50 Hz/1 MHz	8,5	50
Calcium titanate	20	1 MHz	150	3
Lead zirconate	20	1 MHz	110	30
Magnesium titanate	20/150	50 Hz/1 MHz	14	1/4
Porcelain	20/100	51 Hz/1 MHz	5,5	300/80
Rutile	20	1 MHz/1 GHz	80	3/8
Steatite	20	1 MHz/1 GHz	6	20
Strontium titanate	20	1 MHz	200	5
Strontium zirconate	20	1 MHz	38	3
Crystals (single, inorganic)				
LiF	20/25	1 kHz/10 GHz	8.9/9.1	2
LiCl	20	1 kHz/1 MHz	11.8/11.0	
LiBr	20	1 kHz/1 MHz	13.2/12.1	
LiI	20	1 kHz/1 MHz	16.8/11.0	
NaF	20	1 kHz/1 MHz	5.1/6.0	
NaCl	20/25	1 kHz/10 GHz	6.1/5.9	5
NaBr	20	1 kHz/1 MHz	6.5/6.0	
NaI	20	1 kHz/1 MHz	7.3/6.6	
KF	20	1 kHz/1 MHz	5.3/6.0	
KCl	20	1 kHz/10 GHz	4.9/4.8	
KBr	20/25	1 kHz/10 GHz	5.0/4.9	2/7

KI	20	1 kHz/1 MHz	5.1/5.0	
RbF	20	1 kHz	6,5	
RbCl	20	1 kHz	4,9	
RbBr	20	1 kHz	4,9	
RbI	20	1 kHz	4,9	
Calcite	20	1 kHz/10 kHz	8,5	
Diamond	20	500 Hz/100 MHz	5.7/5.5	
Fluorite	20	10 kHz/2 MHz	7.4/6.8	
Gallium Arsenide	20	1 kHz	12	
Germanium	20	1 kHz	16.3	
Iodine	17/22	100 MHz	4.0	
Mica, muscovite	20/100	50 Hz/100 MHz	7.0	
Periclase	25	100 Hz/100 MHz	9,7	3
Quartz	20/25	1 kHz/35 MHz	4.43/4.43	−/0.4
Ruby	17/22	10 kHz	13,3	
Rutile	20	50 Hz/100 MHz	86	100/2
Sapphire	20	50 Hz/1 GHz	9,4	2
Selenium	17/22	100 MHz	6,6	
Silicon	20	1 kHz	11.7	
Sulphur	25	1 kHz	3,8	5
Urea	17/22	400 MHz	3,5	
Zircon	17/22	100 MHz	12	
Glasses				
Borosilicate	20	1 kHz/1 MHz	5,3	50/40
Fused quartz	20/150	50 Hz/100 MHz	3,8	10
Lead	20	1 kHz/1 MHz	6,9	17/13
Soda	20	1 MHz/100 MHz	7,5	100/80
Minerals				
Amber	20	1 MHz/3 GHz	2.8/2.6	
Asbestos (chrysotile)	25	50 Hz/1 MHz	5.8/3.1	1800/250
Bitumen	25	50 Hz/100 MHz	2.7/2.55	60/10
Granite	20	1 MHz	8	
Gypsum	20	10 kHz	5,7	
Marble	20	1 MHz	8	400
Sand	20	1 MHz	2,5	
Sandstone	20	1 MHz	10	

Soil	20	1 MHz	3	
Sulphur	20	3 GHz/10 GHz	3,4	0,5
Paper and Pressboard				
Kraft (tissue)	20/90	1 kHz	1,8	
Rag (cotton)	20/91	50 Hz/50 kHz	1,7	
Pressboard	20	50 Hz	3,2	80
Plastics (non-polar,synthetic)				
Polyethylene	20	50 Hz/1 GHz	2,3	2/3
Polyisobutylene	20	50 Hz/3 GHz	2,2	2/5
Poly4-methylpentene	20	100 Hz/10 kHz	2,1	2
Polyphenyloxide	25	100 Hz/1 MHz	2,6	4/7
Polypropylene	20	50 Hz/1 MHz	2,2	5
Polystyrene	20	50 Hz/1 GHz	2,6	2/5
Polytetrafluoroethylene	20	50 Hz/3 GHz	2,1	2
Plastics (polar,synthetic)				
Polyamides	20	50 Hz/100 MHz		200
Polycarbonates	20	50 Hz/1 MHz	3.2/3.0	10/100
Polyethyleneterephthalateimides	20	1 MHz	3,4	
Polyvinylcarbazole	20	50 Hz/100 MHz	2,8	0,5
Polyvinylchloride	20	50 Hz/100 MHz	3.2/2.8	200/100
Plastics (miscellaneous)				
Aniline resin	20	3 GHz	3,5	500
Cellulose acetate	20	1 MHz/1 GHz	3,5	300/400
Cellulose triacetate	20	50 Hz/100 MHz	3.8/3.2	100/300
Ebonite	20	1 kHz/1 GHz	4.1/3.8	90/30
Epoxy resin	25	1 kHz/100 MHz	3.6/3.5	200
Melamine resin	20	3 GHz	4,7	400
Phenolic resin	20	1 MHz	5,5	500
Urea resin	20	1 MHz	6	300
Vinyl acetate (poly-)	20	1 MHz/10 MHz	4	500
Vinyl chloride (poly-)	20	1 MHz/10 MHz	4	600
Rubbers				

Natural	20/80	1 MHz/10 MHz	2,4	15/100
Butadiene/styrene	20/80	50 Hz/100 MHz	2,5	
Butyl	20	50 Hz/100 MHz	2,4	35/10
Chloroprene	20	1 kHz/1 MHz	6.5/5.7	300/900
Silicone	20	50 Hz/100 MHz	8.6/8.5	50/10
Waxes, etc.				
Chlornaphthalene	20	50 Hz/100 MHz	5.4/4.2	
Ozokerite	20	50 Hz/100 MHz	2,3	0,5
Paraffin wax	20	1 MHz/1 GHz	2,2	2
Petroleum jelly	20/60	50 Hz	2.1/1.9	
Rosin	20	3 GHz	2,4	6
Wood (% water)				
Balsa 0%	20	50 Hz/3 GHz	1.4/1.2	40/140
Beech 16%	20	1 MHz/100 MHz	9.4/8.5	580/830
Birch 10%	20	1 MHz/100 MHz	3,1	400/800
Douglas fir 11%	15	1 MHz/10 MHz	3,2	520/810
Scots pine 15%	20	1 MHz/100 MHz	8.2/7.3	590/940
Walnut 0%	20	10 MHz	2	350
Walnut 17%	20	10 MHz	10	1400
Whitewood 10%	20	1 MHz/100 MHz	3	400/750

Table A.2. Liquids

Material	Temparature (°C)	Frequency	Relative Permittivity (εr')	Conductivity (σ)
Castor oil	20	1 kHz	4,5	
Chlordiphenyl	−10/100	50 Hz/20 kHz	1,4	
Parafin oil	20	1 kHz	2,2	1
Silicone fluid	20	50 Hz/3 GHz	2,2	
Transformer oil	20	50 MHz/100 GHz	2,2	1/42
Alcohols (primary)				
Methanol	25	above 10 GHz	32,65	
Ethanol	25	above 10 GHz	24,51	
Propanol	25	above 10 GHz	20,51	
Butanol	25	above 10 GHz	17,59	
Pentanol	25	above 10 GHz	15,09	
Hexanol	25	above 10 GHz	13,3	
Hydrocarbons				
n-Pentane	20	above 10 GHz	1,84	
n-Hexane	20	above 10 GHz	1,89	
n-Heptane	20	above 10 GHz	1,92	
n-Octane	20	above 10 GHz	1,95	
n-Nonane	20	above 10 GHz	1,97	
n-Decane	20	above 10 GHz	1,99	
n-Undecane	20	above 10 GHz	2,00	
n-Dodecane	20	above 10 GHz	2,01	
Benzene	20	above 10 GHz	2,284	
Cyclopentane	20	above 10 GHz	1,96	
Cyclohexane	20	above 10 GHz	2,025	
Toulene	20	above 10 GHz	2,39	
(Chloro/Fluoro)-hydrocarbons				
CCl_4	20	above 10 GHz	2,24	
CCl_3F	29	above 10 GHz	2,28	
CCl_2F_2	29	above 10 GHz	2,13	

$CClF_3$	−30	above 10 GHz	2,3	
$CHCl_3$	20	above 10 GHz	4,80	
$CHCl_2F$	28	above 10 GHz	5,34	
$CHClF_2$	24	above 10 GHz	6,11	
$(—CCl_2F)_2$	25	above 10 GHz	2,52	
$(—CClF_2)_2$	25	above 10 GHz	2,26	
$(—CH_2Cl)_2$	20	above 10 GHz	10,66	
$(=CCl_2)_2$	25	above 10 GHz	2,3	
$CCl_2=CHCl$	20	above 10 GHz	3,4	
F-pentane	20	above 10 GHz	4,25	
Material	**Temparature (°C)**	**Frequency**	**Relative Permittivity (εr')**	**Conductivity (σ)**
F-benzene	25	above 10 GHz	5,42	
Cl-benzene	20	above 10 GHz	5,70	
Miscellaneous				
Aniline	20	above 10 GHz	6,89	
Acetone	25	above 10 GHz	20,7	
Diethylketone	20	above 10 GHz	17	
Diethylether	20	above 10 GHz	4,34	
Cyclohexanone	20	above 10 GHz	18,3	
Nitrobenzene	25	above 10 GHz	34,8	
CS_2	20	above 10 GHz	2,64	
Liquid gases **Temparature is Kelvin (K)**				
Argon	82	above 10 GHz	1,53	
Helium	4,19	above 10 GHz	1,048	
Hydrogen	20,4	above 10 GHz	1,22	
Nitrogen	70	above 10 GHz	1,45	
Oxygen	80	above 10 GHz	1,5	

Table A.3. Gases

Material	Temparature (°C)	Frequency	Relative Permittivity (10^4 (εr − 1))	Conductivity (σ)
Air dry	20		5,36	
Nitrogen	20		5,47	
Oxygen	20		4,94	
Argon	20		5,17	
Hydrogen	0		2,72	
Deuterium	0		2,69	
Helium	0		0,7	
Neon	0		1,3	
Carbon dioxide	20		9,21	
Carbon monoxide	25		6,4	
Nitrous oxide	25		10,3	
Ethylene	25		13,2	
Carbon disulphide	29		29	
Benzene	100		32,7	
Methanol	100		57	
Ethanol	100		78	
Ammonia	1		71	
Sulphur dioxide	22		82	
Water	100		60	

REFERENCES

1. Stüber, Gordon L.,"Principles of Mobile Communication"; 2nd Edition ,USA, KluwerAcademic Publishers, 2002, pp103-111

2. Wofle, G – Wertz, P – Landstorfer, F.M.: Performance, Accuracy, and Generalization Capability of Indoor Propagation Models in Different Types of Buildings, 10th IEEE Internet Symposium on Personal, Indoor and Mobile Radio Communications (PIMRC) 1999, Sept. 1999, Osaka, Japan F5-2

3. EMC (Electromagnetic Compatibility) Definition. http://www.transpower.co.nz/?id=5326

4. Definition of the picocell. http://whatis.techtarget.com/definition/picocell.html

5. Lempiäinen, J., Manninen, M.; "Radio Interface System Planning For GSM/GPRS/UMTS" ,USA, Kluwer Academic Publishers, 2002, pp94-133

6. W. L. Stutzman and G. A. Thiele, *Antenna Theory and Design.* NewYork: Wiley, 1981, pp. 229-235.

7. Definition of the surface and the ground waves. http://www.tpub.com/content/neets/14182/css/14182_76.htm

8. CAHIT CANBAY 05/12/05 Electromagnetic Wave Lecture Notes

9. THEODORE RAPPAPORT, DEC 31, 2001 Wireless Communications: Principles and Practice, 2nd Edition

10. Modern Approachesin Modeling of Mobile Radio SystemsPropagation Environment",Aleksander Neskovic,Natasa Neskovic, and George Paunovic, University of Belgrade; IEEE Communications Surveys&Tutorials, http://www.comsoc.org/livepubs/surveys/public/3q00issue/neskovic.html;accessdate: 22/05/06

11. Kraus J.D. and D.A. Fleisch Electromagnetics with Applications, Mc Graw-Hill Singapore.1999

12. Ramo, S., J. R. Whinnery, and T. Van Duzer, Fields and Waves in Communication Electronics, Second Edition, John Wiley & Sons Inc., 1984.

13. Bertoni, H. L., Radio Propagation for Modern Wireless Systems, Prentice Hall PTR, New Jersey, 2000.

14. Roger F. Harrington, Time Harmonic Electromagnetic Fields 1993

15. Saunders, S. R., Antennas and Propagation for Wireless Communication Systems, J. Wiley & Sons, New York, 1999

16. Jean-Paul M.G. Linnartz , Rician Fading 2009, http://www.wirelesscommunication.nl/reference/chaptr03/ricepdf/rice.htm

17. Jean-Paul M.G. Linnartz, Fading 2009, http://www.wirelesscommunication.nl/reference/chaptr03/fading/delayspr.htm

18. S.Hudson, Indoor Radio Propagation at 915MHz., RF Engineering For Telecommunication, Agilent Technologies, USA, Available at www.educatorscorner.com/media/Exp94e.pdf.

19. Richard Fitzpatrick , Mie Scattering Lecture Notees, 2002-05-18, http://farside.ph.utexas.edu/teaching/jk1/lectures/node103.html